

Article

Synthesis, Anti-Tyrosinase Activity, and Spectroscopic Inhibition Mechanism of Cinnamic Acid–Eugenol Esters

 Jianping Li ¹, Xiaofeng Min ¹, Xi Zheng ¹, Shaohua Wang ², Xuetao Xu ^{1,*}  and Jinbao Peng ^{1,*}
¹ School of Biotechnology and Health Sciences, Wuyi University, Jiangmen 529020, China; wyuchemxzh@126.com (X.Z.)

² School of Pharmacy, Lanzhou University, Lanzhou 730000, China; wangshh@lzu.edu.cn

* Correspondence: wyuchemxxt@126.com (X.X.); pengjb_05@126.com (J.P.)

Abstract: Tyrosinase plays crucial roles in mediating the production of melanin pigment; thus, its inhibitors could be useful in preventing melanin-related diseases. To find potential tyrosinase inhibitors, a series of cinnamic acid–eugenol esters (c1~c29) was synthesized and their chemical structures were confirmed by ¹H NMR, ¹³C NMR, HRMS, and FT-IR, respectively. The biological evaluation results showed that all compounds c1~c29 exhibited definite tyrosinase inhibitory activity; especially, compound c27 was the strongest tyrosinase inhibitor (IC₅₀: 3.07 ± 0.26 μM), being ~4.6-fold stronger than the positive control, kojic acid (IC₅₀: 14.15 ± 0.46 μM). Inhibition kinetic studies validated compound c27 as a reversible mixed-type inhibitor against tyrosinase. Three-dimensional fluorescence and circular dichroism (CD) spectra results indicated that compound c27 could change the conformation and secondary structure of tyrosinase. Fluorescence-quenching results showed that compound c27 quenched tyrosinase fluorescence in the static manner with one binding site. Molecular docking results also revealed the binding interactions between compound c27 and tyrosinase. Therefore, cinnamic acid–eugenol esters, especially c27, could be used as lead compounds to find potential tyrosinase inhibitors.

Keywords: tyrosinase; inhibitors; cinnamic acid; eugenol; hybrid



Citation: Li, J.; Min, X.; Zheng, X.; Wang, S.; Xu, X.; Peng, J. Synthesis, Anti-Tyrosinase Activity, and Spectroscopic Inhibition Mechanism of Cinnamic Acid–Eugenol Esters. *Molecules* **2023**, *28*, 5969. <https://doi.org/10.3390/molecules28165969>

Academic Editor: Pierangela Ciuffreda

Received: 19 July 2023

Revised: 2 August 2023

Accepted: 5 August 2023

Published: 9 August 2023



Copyright: © 2023 by the authors. Licensee MDPI, Basel, Switzerland. This article is an open access article distributed under the terms and conditions of the Creative Commons Attribution (CC BY) license (<https://creativecommons.org/licenses/by/4.0/>).

1. Introduction

Tyrosinase (EC 1.14.18.1), which is one kind of copper-containing metalloenzyme, widely exists in nature animals and plants [1–3]. Tyrosinase plays crucial roles in mediating the production of melanin pigment via two steps [4–8]. In the melanin process, tyrosinase monophenolase firstly catalyzes the hydroxylation of L-tyrosine to yield L-DOPA, which is further oxidized into *o*-dopaquinone by tyrosinase diphenolase (Figure 1) [9–12]. The produced melanin is distributed in the keratinocytes of human skin and hair; it is very important for human health [13–17], due to the effects of melanin in protecting human skin and eyes from damage against UV light [18,19]. However, overproduction of melanin results in epidermal pigmentation, thereby causing skin hyperpigmentation disorders, including melasma, age spots, and freckles [20–22]. Inhibiting tyrosinase activity can reduce the formation of melanin; thereby, tyrosinase inhibitors can be utilized to prevent melanin-related diseases [23,24]. In addition, tyrosine inhibitors also can be utilized as effective food preservatives to delay food browning [25–27].

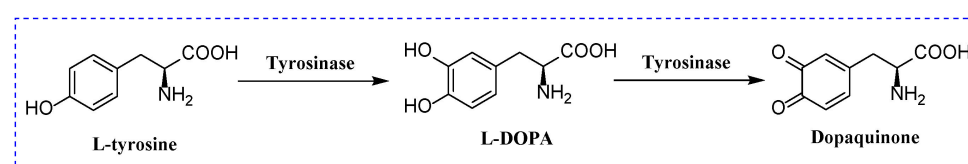


Figure 1. Reaction process involving tyrosinase as a catalytic protein.

Up to now, numerous natural and synthetic tyrosinase inhibitors have been reported [28–32], but only a few are used to prevent melanin production, such as kojic acid and hydroquinone (Figure 2), in spite of their instability and undesirable side effects. The abovementioned problems have prompted researchers to finding potential tyrosinase inhibitors to improve human health.

It is widely known that natural products are an important source for new drug development, and many clinical drugs are derived from natural products. Nowadays, many natural compounds have been verified to have tyrosinase inhibitory activity [33–36]. For example, cinnamic acid (Figure 2) is one important active ingredient of *Cinnamomum cassia* Presl and its derivatives promise potential tyrosinase activity [37], as well as other pharmacological activities, including antiviral [38], anti-inflammatory [39], antitumor [40], antibacterial [41], and antileishmanial activities [42] (Figure 2). Although cinnamic acid has been used in the food and medicine industries, its moderate tyrosinase inhibitory activity limits its wider application, so it is necessary to optimize cinnamic acid's structure to enhance its tyrosinase inhibitory activity. Now, many cinnamic acid derivatives, especially cinnamic acid esters, are being designed as potential tyrosinase inhibitors [43–45] (Figure 2). Analyzing the above structure, it can be seen that esterification modification of cinnamic acid would be a feasible strategy to obtain better tyrosinase inhibitors, and esterification modification of the phenolic hydroxyl group would be better than a structure with an alkane chain as the bridge.

Eugenol (Figure 2), one primary bioactive component of *Eugenia caryophyllata* Thunb, has shown certain tyrosinase inhibitory and antioxidant activities [46]. Cinnamic acid–eugenol esters with an alkane chain bridge have been synthesized as tyrosinase inhibitors [47] (Figure 2). Thus, we inferred that esterification modification of cinnamic acid with the phenolic hydroxyl group of eugenol would obtain more active tyrosinase inhibitors. From preliminary docking studies, a skeleton compound was bound into the active pocket with the benzene ring of cinnamic acid, close to the copper ions, and formed hydrophobic interactions with Met257, Val248, Val283, and Ala286 (Figure 2), with the aim of enhancing the binding of compound with tyrosinase. These results evidenced our idea of introducing eugenol into the parental cinnamic acid.

In addition, hybrids of pharmacophoric moieties have been an important part of the strategy to design new compound molecules with increased affinity and efficacy [24,48]. Therefore, as part of our ongoing efforts to find more potential tyrosinase inhibitors, the hybrids of the natural products cinnamic acid and eugenol were synthesized, followed by anti-tyrosinase activity screening, spectroscopic mechanism investigation, and a docking study.

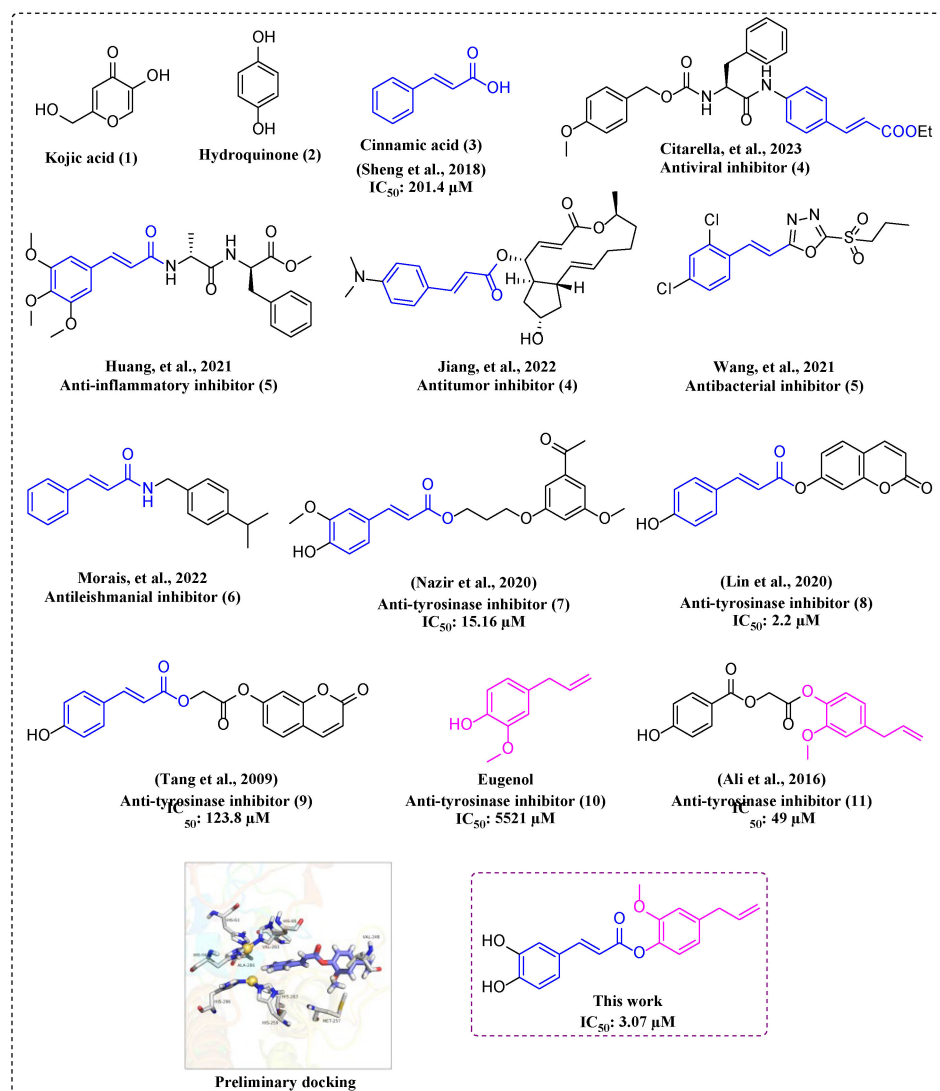
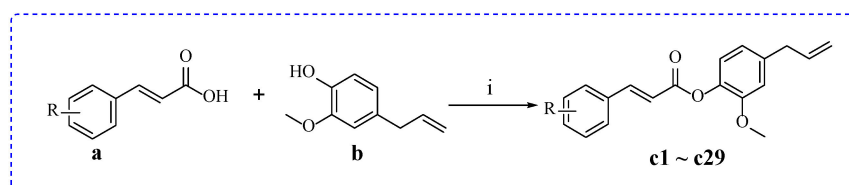


Figure 2. The structures of cinnamic acid, eugenol, and their derivatives, and preliminary docking [37–45,47].

2. Results and Discussion

2.1. Chemistry

Cinnamic acid–eugenol esters **c1**–**c29** were conveniently synthesized using substituted cinnamic acids (a) and eugenol (b) as materials under EDCI/DMAP-mediated coupling, and the synthetic route is listed in Scheme 1. The structures of all compounds (**c1**–**c29**) were identified by FT-IR, ^1H NMR, ^{13}C NMR, and HRMS.



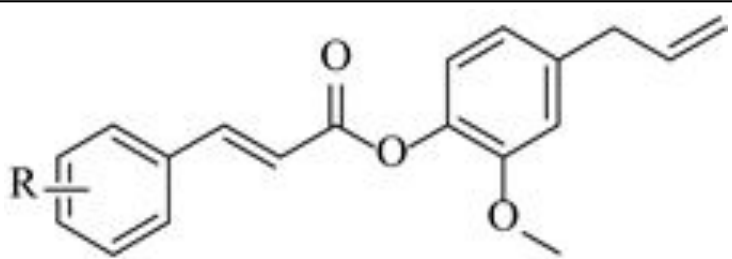
Scheme 1. Synthesis of cinnamic acid–eugenol esters **c1**–**c29**. Reagents and conditions: (i) substituted cinnamic acids, eugenol, EDCI, DMAP, DCM, 0 $^{\circ}\text{C}$ –rt.

2.2. Tyrosinase Inhibitory Activity

The tyrosinase inhibitory activities of cinnamic acid–eugenol esters **c1**–**c29** were screened using L-DOPA as a substrate. We firstly screened their tyrosinase inhibition

rates at a compound concentration of 64 μM . As presented in Table 1, most synthesized cinnamic acid–eugenol esters showed potential tyrosinase inhibitory activity. Among them, compounds **c14**, **c15**, and **c27** showed stronger inhibitory activities, with inhibition rates of 67.61%, 76.14%, 81.46%, while other compounds presented lower inhibition rates. Then, the 50% inhibitory concentration (IC_{50}) values of compounds **c14**, **c15**, and **c27** were also investigated. As shown in Table 1, compound **c27** showed the strongest inhibitory activity, with an IC_{50} value of $3.07 \pm 0.28 \mu\text{M}$, which was stronger than that of cinnamic acid ($\text{IC}_{50} = 201.4 \pm 5.3 \mu\text{M}$), eugenol ($\text{IC}_{50} = 5521 \pm 25 \mu\text{M}$), and the positive control, kojic acid ($\text{IC}_{50} = 14.15 \pm 0.46 \mu\text{M}$). The inhibitory activity results showed that the hybrids of cinnamic acid and eugenol, especially compound **c27**, showed stronger activities than the parent compound of cinnamic acid and eugenol, suggesting that the hybrid of cinnamic acid and eugenol might be an effective strategy to find potential tyrosinase inhibitors.

Table 1. Tyrosinase inhibitory activities of cinnamic acid esters **c1**–**c29**.



Compounds	R	Inhibition Rate at 64 μM (%)	IC_{50} (μM)
c1	-H	12 \pm 1	-
c2	-2CH ₃	12 \pm 0.3	-
c3	-3CH ₃	39 \pm 3	-
c4	-4CH ₃	15 \pm 1	-
c5	-2Cl	29 \pm 3	-
c6	-3Cl	17 \pm 2	-
c7	-4Cl	24 \pm 1	-
c8	-2F	17 \pm 3	-
c9	-3F	17 \pm 3	-
c10	-4F	17 \pm 1	-
c11	-2Br	10 \pm 0.4	-
c12	-3Br	3 \pm 0.8	-
c13	-4Br	13 \pm 1	-
c14	-3OH	68 \pm 0.7	16.28 \pm 1.52
c15	-4OH	76 \pm 0.2	5.95 \pm 1.46
c16	-2NO ₂	5 \pm 0.1	-
c17	-3NO ₂	9 \pm 0.8	-
c18	-4NO ₂	14 \pm 1	-
c19	-2CH ₃ O	3 \pm 0.2	-
c20	-3CH ₃ O	3 \pm 0.1	-
c21	-4CH ₃ O	7 \pm 0.9	-
c22	-2CF ₃	6 \pm 0.5	-
c23	-3CF ₃	5 \pm 0.2	-
c24	-4CF ₃	2 \pm 0.1	-
c25	-(CH ₃ CH ₂) ₂ N	26 \pm 1	-
c26	-3CH ₃ O, -4OH	47 \pm 1	-
c27	-3,4OH	81 \pm 2	3.07 \pm 0.28
c28	-3F, -4Cl	19 \pm 0.2	-
c29	-3,4CH ₂ O	4 \pm 1	-
Cinnamic acid			201.4 \pm 5.3
Eugenol			5521 \pm 25
Kojic acid		76 \pm 2	14.15 \pm 0.46

"-" mean not detected.

Moreover, it also was observed that the introduction of substituents group in the benzene ring of cinnamic acid resulted in a change of tyrosinase inhibitory activity. Especially, the introduction of the phenolic hydroxyl group (**c14**, **c15**, **c26**, and **c27**) obviously increased tyrosinase inhibitory activity. In particular, compound **c27** with the 3,4-diphenol hydroxy group was the most active compound (IC_{50} : $3.07 \pm 0.28 \mu\text{M}$), being ~ 4.6 -fold stronger than kojic acid (IC_{50} : $14.15 \pm 0.46 \mu\text{M}$). These results showed that the introduction of the phenolic hydroxyl group might be essential for tyrosinase inhibitory activity, which is consistent with previous research results [36–38]. However, the introduction of non-hydroxy substituents, including methyl, chlorine, fluorine, bromine, nitro, methoxy, and trifluoromethyl, had no obvious effect in improving this activity.

2.3. Kinetic Study

Inhibition kinetic studies were assayed to analyze the potential inhibition mechanism of compound **c27** toward tyrosinase. Figure 3A displays the relationship between the tyrosinase concentration with residual enzyme activity under compound **c27** (0–4 μM), which shows straight lines passing through the origin with different slopes. Therefore, compound **c27** was identified as a reversible inhibitor [49,50]. Figure 3B shows the Lineweaver–Burk plots of substrate concentration and residual enzyme activity under compound **c27** (0–4 μM). It could be observed that all lines with different slopes intersected in the second quadrant, suggesting compound **c27** is a mixed-type inhibitor [51,52].

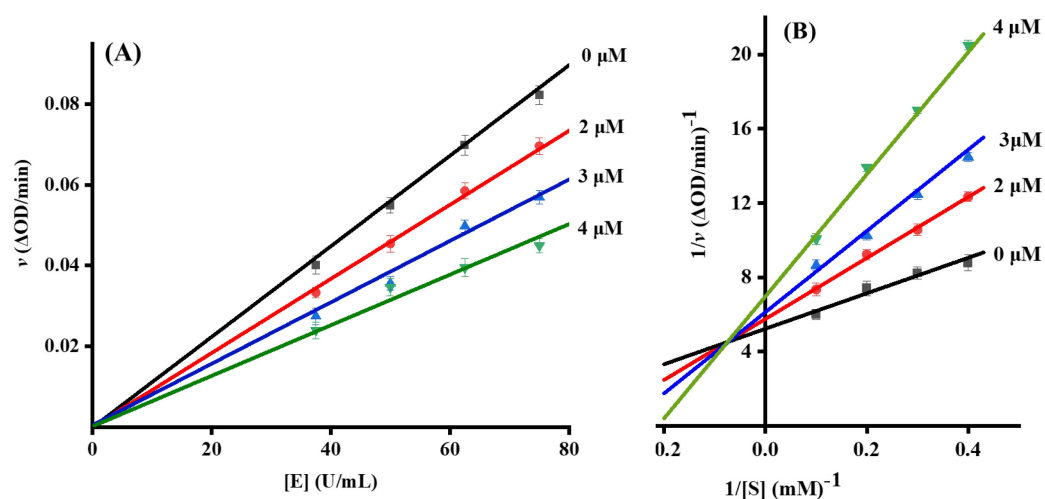


Figure 3. (A) The plots of v versus $[E]$ under compound **c27**; (B) Lineweaver–Burk plots of v versus $[S]$ under compound **c27**.

2.4. Three-Dimensional Fluorescence Spectra

To better understand the inhibition mechanisms, the conformational change of tyrosinase by compound **c27** was monitored using a 3D fluorescence spectrum. As shown in Figure 4A, two characteristic peaks appeared, peak 1 ($\lambda_{\text{ex}}/\lambda_{\text{em}} = 280 \text{ nm}/340 \text{ nm}$) and peak 2 ($\lambda_{\text{ex}}/\lambda_{\text{em}} = 230 \text{ nm}/335 \text{ nm}$), corresponding to Tyr and Trp residues, and a polypeptide strand transition, respectively. Figure 4B shows the 3D fluorescence spectrum of the tyrosinase–compound **c27** mixture. It could be observed that treatment of compound **c27** reduced the intensity of peak 1 and peak 2 by 21.47% and 32.71%, respectively. These results suggest that compound **c27** could change the conformation of tyrosinase to inhibit its activity.

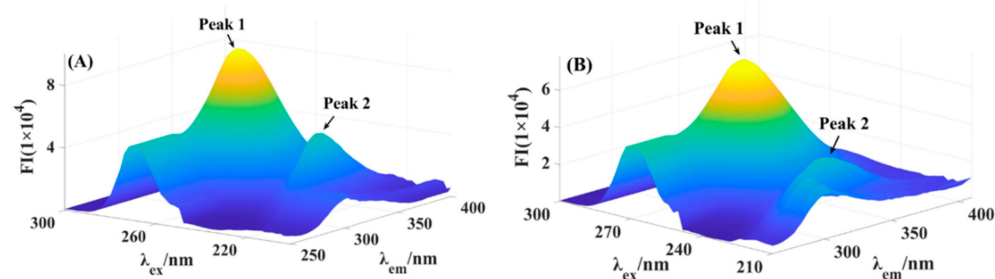


Figure 4. (A) Three-dimensional fluorescence spectra of tyrosinase. (B) Three-dimensional fluorescence spectra of tyrosinase with compound **c27**.

2.5. Circular Dichroism Spectra

The CD spectra were also used to analyze the effects of compound **c27** on the secondary structure of tyrosinase. Figure 5 presents the CD spectra of tyrosinase–compound **c27** mixtures, which showed characteristic negative bands at 205–230 nm owing to the electronic transition of the α -helix peptide. Treatment of compound **c27** resulted in the reduction of band intensity, indicating the conformation change of tyrosinase by compound **c27**. The secondary structure contents of tyrosinase are listed in Table 2, which evidences that treatment of compound **c27** (molar ratios: 3:1) caused the increase of the α -helix (from 7.10% to 9.85%), β -sheet (from 48.90% to 49.27%), and β -turn (from 17.21% to 18.55%), but the decrease of the random coil (from 28.40% to 27.94%).

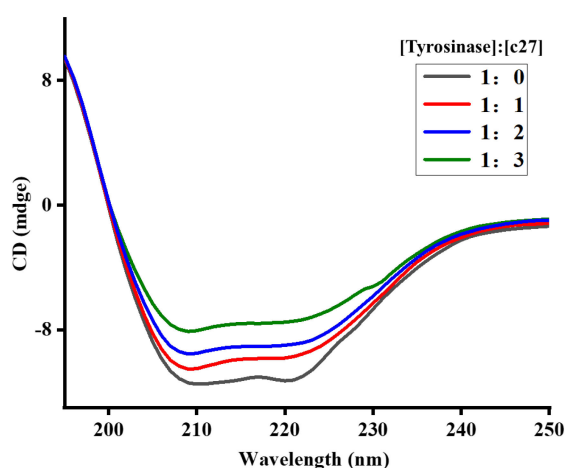


Figure 5. Circular dichroism spectra of the tyrosinase and compound **c27** system.

Table 2. The secondary structures contents of tyrosinase.

[Tyrosinase]:[c27]	α -Helix (%)	β -Sheet (%)	β -Turn (%)	Random Coil (%)
1:0	7.10	48.90	17.21	28.40
1:1	7.12	49.00	17.63	28.23
1:2	9.56	49.23	18.37	28.12
1:3	9.85	49.27	18.55	27.94

2.6. Fluorescence Quenching

Fluorescence quenching was performed to analyze the interactions between compound **c27** and tyrosinase. As shown in Figure 6A–C, the fluorescence spectra of tyrosinase at 304, 307, and 310 K reduced continuously with the titration addition of compound **c27** (0–4.5 μ M), but the peak position did not shift. This phenomenon shows that the interaction of compound **c27** with tyrosinase could quench tyrosinase intrinsic fluorescence. The Stern–Volmer plots (Figure 6D) at 304, 307, and 310 K obtained from fluorescence quenching data showed good linearity, demonstrating a onefold quenching type.

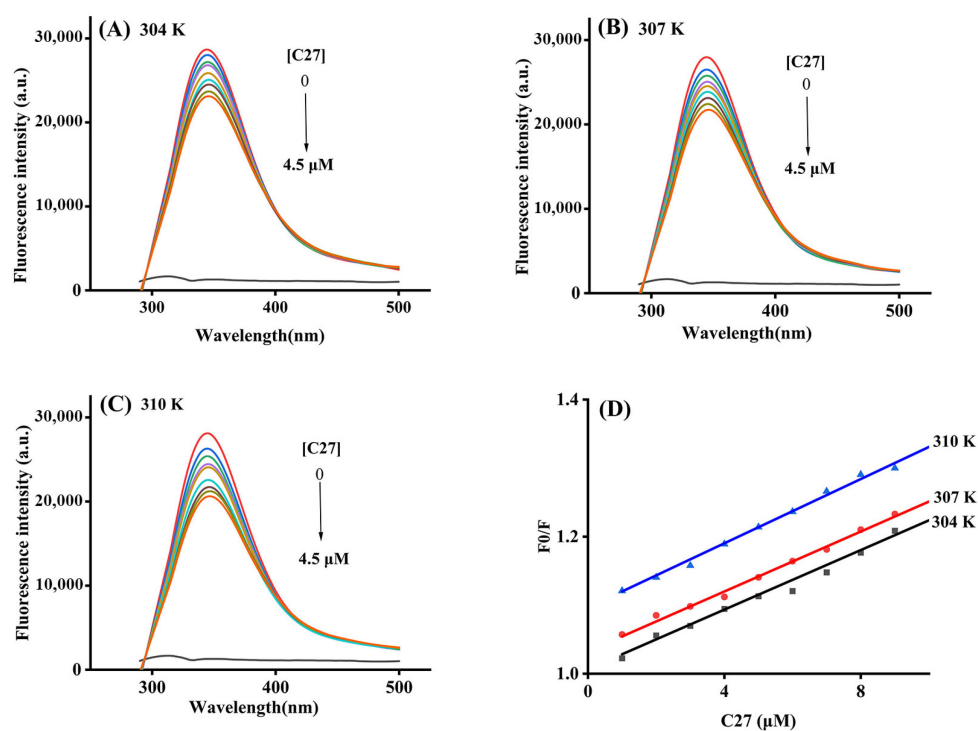


Figure 6. Fluorescence quenching of tyrosinase by compound **c27**. (A) 304 K; (B) 307 K; (C) 310 K; (D) Stern–Volmer plots.

To clarify the quenching mechanism, the relevant quenching constants were determined (Table 3). The Stern–Volmer quenching constant (K_{SV}) values presented declined with the increasing temperature, and the quenching rate constant (K_q) values all reached the order of magnitude of 10^{12} , suggesting a static quenching process. Furthermore, the binding constant (K_a) values (order of magnitude of 10^4) suggested a moderate binding between compound **c27** and tyrosinase and the number of binding sites (n) was revealed as only one.

Table 3. Quenching constants of tyrosinase with compound **c27**.

T (K)	K_{SV} ($\times 10^4$ L·mol $^{-1}$)	K_q ($\times 10^{12}$ L·mol $^{-1}$)	K_a ($\times 10^4$ L·mol $^{-1}$)	n
304	4.77	4.77	0.05	0.59
307	4.32	4.32	0.93	0.86
310	4.29	4.29	3.85	0.99

2.7. Molecular Docking

Molecular docking was introduced to analyze the binding interaction between compound **c27** and tyrosinase, using SYBYL software. To validate the docking protocol and better understand the binding interaction of compound **c27**, analyses of the dockings of the tyrosinase (2Y9X) ligand tropolone, control kojic acid, and substrate L-DOPA with tyrosinase were also conducted, and the results are presented in Figure 6. As shown in Figure 7A,B, compound **c27**, tropolone, kojic acid, and L-DOPA were all anchored at about the same position of the active site; especially, the hydroxyl group of each compound was close to two copper ions (2.0–3.7 Å). Tropolone formed one hydrogen bond with His259 (2.9 Å) (Figure 7C), while kojic acid formed one hydrogen bond with His280 (1.9 Å) and hydrophobic interactions with His263, Val283, and Ala286 (Figure 7D). Analysis of compound **c27** (Figure 7E) showed its one phenolic hydroxyl group formed a hydrogen bond with His259 (2.6 Å), methoxy and ester groups both formed one hydrogen bond with Val283 (2.3 Å and 2.3 Å), and compound **c27** had a hydrophobic interaction with Leu275, Pro277,

and Pro284, respectively. In the docking of L-DOPA (Figure 7F), there were two hydrogen bonds with His61 (2.3 Å) and Asn260 (2.1 Å), and hydrophobic interaction with His263, Val283, and Ala286. For compound **c27** and L-DOPA, the catechol rings of cinnamic acid fraction and L-DOPA were both inserted inside the cavity and located at about the same distance from two copper ions (2.0, 2.1, 3.0, 3.6 Å vs. 2.0, 2.9, 3.6, 3.7 Å). In contrast to the cinnamic acid fraction, the eugenol fraction of compound **c27** was out of the cavity. Analysis of the above interactions helps to clarify the interactions between compound **c27** and tyrosinase.

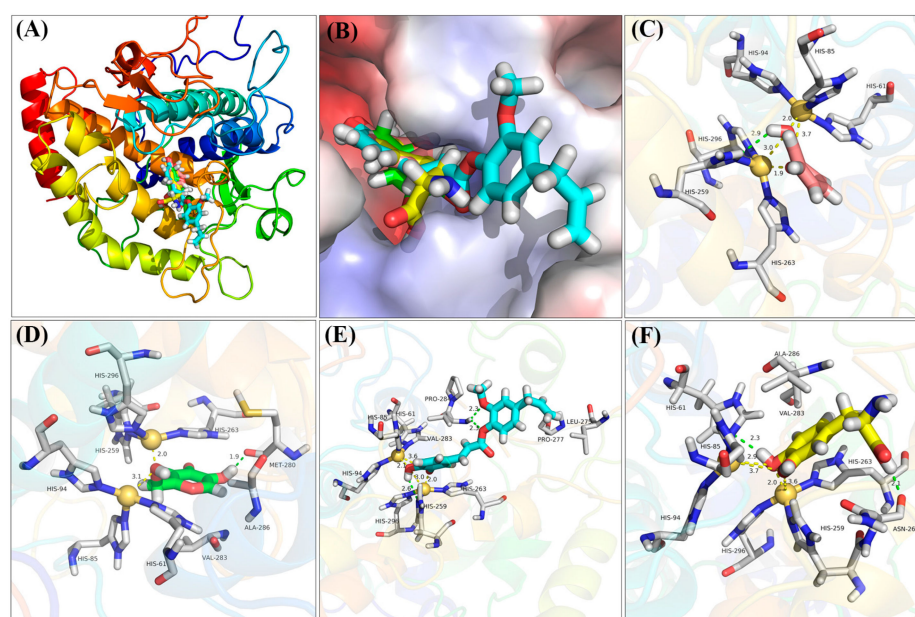


Figure 7. (A,B) The binding conformation of compound **c27**, tropolone, kojic acid, and L-DOPA in active pocket. (C) Detailed binding of tropolone with tyrosinase. (D) Detailed binding of kojic acid with tyrosinase. (E) Detailed binding of compound **c27** with tyrosinase. (F) Detailed binding of L-DOPA with tyrosinase.

2.8. Drug-like Properties

The drug-like properties of compound **c27** were analyzed using SwissADME online software (<https://www.swissadme.ch/index.php>, accessed on 1 July 2023). As shown in Table 4, compound **c27** had favorable drug-like properties with good MW, RB, HBA, HBD, and TPSA values, except poor water solubility.

Table 4. Drug-like properties of compound **c27**.

MF	MW	RB	HBA	HBD	PPSA	Log Po/w	WS
C ₁₉ H ₁₈ O ₅	326.34	7	5	2	75.99	3.10	Poorly

MF (molecular formula), MW (molecular weight, g/mol), RB (rotatable bonds), HBA (H-bond acceptor atoms), HBD (H-bond donor atoms), TPSA (topology polar surface area, Å²), WS (water solubility).

3. Materials and Methods

3.1. Materials

Tyrosinase mushroom and L-DOPA were supplied by Sigma-Aldrich (St. Louis, MI, USA). All other reagents were commercially available. ¹H NMR and ¹³C NMR spectra were recorded on a Bruker 500 MHz NMR spectrometer instrument (Billerica, MA, USA). High-resolution mass spectral analysis (HRMS) data were measured on the Apex II by means of the ESI technique.

3.2. Methods

3.2.1. Synthesis of Cinnamic Acid–Eugenol Ester Derivatives (c1~c29)

Substituted cinnamic acid (1.4 mmol), eugenol (1 mmol), EDCI (2 mmol), and DMAP (1.2 mmol) were added into anhydrous DCM (10 mL) under an ice bath and stirred for 30 min. Then, the mixture was stirred at room temperature until the reaction completed. Afterwards, it was quenched with water (30 mL) and the mixture was extracted with DCM (15 mL \times 3). The merged organic layers were washed with saturated sodium chloride (30 mL \times 3), followed by drying with anhydrous sodium sulfate, evaporating solvent, and separating by silica gel column to produce the targeted cinnamic acid–eugenol ester derivatives (c1~c29).

4-allyl-2-methoxyphenyl cinnamate (c1). White solid; yield 68% (the crude was purified using a mixture of PE/EtOAc 100:1); mp: 254.2–255.9 °C; ^1H NMR (500 MHz, CDCl_3) δ 7.88 (d, J = 16.0 Hz, 1H, Ar-H), 7.60 (d, J = 3.9 Hz, 1H, Ar-H), 7.59 (d, J = 2.6 Hz, 1H, CH), 7.43 (s, 1H, Ar-H), 7.42 (s, 2H, Ar-H), 7.04 (d, J = 8.0 Hz, 1H, Ar-H), 6.83 (s, J = 1.9 Hz, 1H, Ar-H), 6.81 (d, J = 8.0 Hz, 1H, Ar-H), 6.69 (d, J = 16.0 Hz, 1H, CH), 5.99 (td, J = 16.9, 6.7 Hz, 1H, CH), 5.17–5.08 (m, 2H, CH_2), 3.84 (s, 3H, OCH_3), 3.41 (d, J = 6.8 Hz, 2H, CH_2); ^{13}C NMR (126 MHz, CDCl_3) δ 165.3 (C=O), 151.1 (Ar-C), 146.6 (CH), 139.1 (Ar-C), 138.1 (CH), 137.2 (Ar-C), 134.4 (Ar-C), 130.7 (Ar-2C), 129.1 (Ar-2C), 128.4 (Ar-C), 122.8 (Ar-C), 120.8 (Ar-C), 117.2 (CH), 116.3 (CH), 112.8 (Ar-C), 56.0 (OCH_3), 40.3 (CH_2); HRMS (ESI-MS) m/z : $[\text{M} + \text{H}]^+$ calcd for $\text{C}_{19}\text{H}_{18}\text{O}_3^+$: 295.1337; found: 295.1326; IR (cm^{-1}): 2937 (OCH_3), 1704 (C=O), 1165 (Ar-C=C).

4-allyl-2-methoxyphenyl (E)-3-(o-tolyl)acrylate (c2). White solid; yield 55% (the crude was purified using a mixture of PE/EtOAc 100:1); mp: 265.1–266.3 °C; ^1H NMR (500 MHz, CDCl_3) δ 8.16 (d, J = 15.9 Hz, 1H, Ar-H), 7.65 (d, J = 7.6 Hz, 1H, Ar-H), 7.31 (t, J = 7.4 Hz, 1H, CH), 7.25 (s, 1H, Ar-H), 7.23 (d, J = 7.2 Hz, 1H, Ar-H), 7.04 (d, J = 7.9 Hz, 1H, Ar-H), 6.83 (s, 1H, Ar-H), 6.81 (d, J = 8.7 Hz, 1H, Ar-H), 6.61 (d, J = 15.9 Hz, 1H, CH), 5.99 (td, J = 16.8, 6.7 Hz, 1H, CH), 5.16–5.09 (m, 2H, CH_2), 3.84 (s, 3H, OCH_3), 3.41 (d, J = 6.7 Hz, 2H, CH_2), 2.48 (s, 3H, CH_3); ^{13}C NMR (126 MHz, CDCl_3) δ 165.3 (C=O), 151.1 (Ar-C), 144.2 (CH), 139.1 (Ar-C), 138.1 (CH), 138.0 (Ar-C), 137.2 (Ar-C), 133.3 (Ar-C), 131.0 (Ar-C), 130.5 (Ar-C), 126.7 (Ar-C), 126.5 (Ar-C), 122.8 (Ar-C), 120.8 (Ar-C), 118.1 (CH), 116.3 (CH), 112.9 (Ar-C), 56.00 (OCH_3), 40.2 (CH_2), 20.0 (CH_3); HRMS (ESI-MS) m/z : $[\text{M} + \text{H}]^+$ calcd for $\text{C}_{20}\text{H}_{20}\text{O}_3^+$: 309.1487; found: 309.1483; IR (cm^{-1}): 2937 (OCH_3), 2967 (CH_3), 1704 (C=O), 1165 (Ar-C=C).

4-allyl-2-methoxyphenyl (E)-3-(m-tolyl)acrylate (c3). Yellow solid; yield 67% (the crude was purified using a mixture of PE/EtOAc 100:1); mp: 326.6–327.8 °C; ^1H NMR (500 MHz, CDCl_3) δ 7.88 (d, J = 16.0 Hz, 1H, Ar-H), 7.44 (s, 1H, Ar-H), 7.42 (s, CH), 7.34 (t, J = 7.8 Hz, 1H, Ar-H), 7.28 (d, J = 9.9 Hz, 1H, Ar-H), 7.07 (d, J = 8.0 Hz, 1H, Ar-H), 6.86 (s, J = 1.9 Hz, 1H, Ar-H), 6.84 (d, J = 8.0 Hz, 1H, Ar-H), 6.70 (d, J = 16.0 Hz, 1H, CH), 6.02 (td, J = 16.8, 6.7 Hz, 1H, CH), 5.22–5.11 (m, 2H, CH_2), 3.87 (s, 3H, OCH_3), 3.44 (d, J = 6.7 Hz, 2H, CH_2), 2.43 (s, 3H, CH_3); ^{13}C NMR (126 MHz, CDCl_3) δ 165.4 (C=O), 151.1 (Ar-C), 146.8 (CH), 139.0 (Ar-C), 138.8 (CH), 138.1 (Ar-C), 137.2 (Ar-C), 134.4 (Ar-C), 131.6 (Ar-C), 129.1 (Ar-C), 129.0 (Ar-C), 125.6 (Ar-C), 122.8 (Ar-C), 120.8 (Ar-C), 117.0 (CH), 116.3 (CH), 112.9 (Ar-C), 56.0 (OCH_3), 40.3 (CH_2), 21.5 (CH_3); HRMS (ESI-MS) m/z : $[\text{M} + \text{H}]^+$ calcd for $\text{C}_{20}\text{H}_{20}\text{O}_3^+$: 309.1487; found: 309.1484; IR (cm^{-1}): 2937 (OCH_3), 2961 (CH_3), 1704 (C=O), 1165 (Ar-C=C).

4-allyl-2-methoxyphenyl (E)-3-(p-tolyl)acrylate (c4). Yellow solid; yield 57% (the crude was purified using a mixture of PE/EtOAc 100:1); mp: 266.8–267.7 °C; ^1H NMR (500 MHz, CDCl_3) δ 7.85 (d, J = 16.0 Hz, 1H, Ar-H), 7.49 (s, 1H, Ar-H), 7.48 (s, 1H, CH), 7.23 (s, 1H, Ar-H), 7.21 (s, 1H, Ar-H), 7.02 (d, J = 7.9 Hz, Ar-H), 6.82 (s, J = 1.9 Hz, 1H, Ar-H), 6.80 (dd, J = 8.1, 1.9 Hz, 1H, Ar-H), 6.63 (d, J = 16.0 Hz, 1H, CH), 5.98 (ddt, J = 16.8, 10.0, 6.7 Hz, 1H, CH), 5.15–5.08 (m, 2H, CH_2), 3.83 (s, 3H, OCH_3), 3.40 (d, J = 6.7 Hz, 2H, CH_2), 2.39 (s, 3H, CH_3); ^{13}C NMR (126 MHz, CDCl_3) δ 165.5 (C=O), 151.2 (Ar-C), 146.6 (Ar-C), 141.2 (Ar-C), 139.0 (CH), 138.1 (Ar-C), 137.2 (Ar-C), 131.7 (Ar-C), 129.8 (Ar-C), 128.4 (Ar-C), 122.8 (Ar-C), 120.8 (Ar-C), 116.3 (CH), 116.1 (CH), 112.9 (Ar-C), 56.0 (OCH_3), 40.3 (CH_2),

21.7 (CH₃); HRMS (ESI-MS) *m/z*: [M + H]⁺ calcd for C₂₀H₂₀O₃⁺: 309.1487; found: 309.1483; IR (cm⁻¹): 2937 (OCH₃), 2968 (CH₃), 1704 (C=O), 1165 (Ar-C=C).

4-allyl-2-methoxyphenyl (E)-3-(2-chlorophenyl)acrylate (c5). White solid; yield 65% (the crude was purified using a mixture of PE/EtOAc 60:1); mp: 247.4–247.7 °C; ¹H NMR (500 MHz, CDCl₃) δ 8.29 (d, *J* = 16.0 Hz, 1H, Ar-H), 7.71 (dd, *J* = 7.4, 2.1 Hz, 1H, Ar-H), 7.44 (d, *J* = 7.6 Hz, 1H, CH), 7.34 (d, *J* = 7.5 Hz, 1H, Ar-H), 7.31 (d, *J* = 7.4 Hz, 1H, Ar-H), 7.04 (d, *J* = 7.9 Hz, 1H, Ar-H), 6.83 (s, *J* = 1.9 Hz, 1H, Ar-H), 6.81 (d, *J* = 8.0 Hz, 1H, Ar-H), 6.67 (d, *J* = 16.0 Hz, 1H, CH), 5.98 (ddt, *J* = 16.8, 10.0, 6.7 Hz, 1H, CH), 5.16–5.09 (m, 2H, CH₂), 3.84 (s, 3H, OCH₃), 3.41 (d, *J* = 6.7 Hz, 2H, CH₂); ¹³C NMR (126 MHz, CDCl₃) δ 164.8 (C=O), 151.1 (Ar-C), 142.2 (CH), 139.2 (Ar-C), 138.0 (CH), 137.2 (Ar-C), 135.3 (Ar-C), 132.6 (Ar-C), 131.45 (Ar-C), 130.4 (Ar-C), 128.0 (Ar-C), 127.3 (Ar-C), 122.7 (Ar-C), 120.9 (Ar-C), 119.8 (CH), 116.3 (CH), 112.9 (Ar-C), 56.0 (OCH₃), 40.2 (CH₂); HRMS (ESI-MS) *m/z*: [M + H]⁺ calcd for C₁₉H₁₇ClO₃⁺: 329.0947; found: 329.0937; IR (cm⁻¹): 2937 (OCH₃), 1704 (C=O), 1165 (Ar-C=C), 726 (Cl).

4-allyl-2-methoxyphenyl (E)-3-(3-chlorophenyl)acrylate (c6). Yellow solid; yield 73% (the crude was purified using a mixture of PE/EtOAc 60:1); mp: 278.3–278.9 °C; ¹H NMR (500 MHz, CDCl₃) δ 7.80 (d, *J* = 16.0 Hz, 1H, Ar-H), 7.57 (s, 1H, Ar-H), 7.45 (d, *J* = 7.4 Hz, 1H, CH), 7.39 (d, *J* = 8.2 Hz, 1H, Ar-H), 7.36 (d, *J* = 7.5 Hz, 1H, Ar-H), 7.03 (d, *J* = 7.9 Hz, 1H, Ar-H), 6.82 (s, 1H, Ar-H), 6.81 (d, *J* = 8.0 Hz, 1H, Ar-H), 6.67 (d, *J* = 16.1 Hz, 1H, CH), 5.98 (td, *J* = 16.8, 6.7 Hz, 1H, CH), 5.15–5.09 (m, 2H, CH₂), 3.83 (s, 3H, OCH₃), 3.40 (d, *J* = 6.7 Hz, 2H, CH₂); ¹³C NMR (126 MHz, CDCl₃) δ 164.9 (C=O), 151.0 (Ar-C), 144.9 (Ar-C), 139.2 (CH), 138.0 (Ar-C), 137.2 (Ar-C), 136.2 (CH), 135.0 (Ar-C), 130.5 (Ar-C), 130.3 (Ar-C), 128.2 (Ar-C), 126.5 (Ar-C), 122.7 (Ar-C), 120.9 (Ar-C), 118.7 (CH), 116.3 (CH), 112.9 (Ar-C), 56.0 (OCH₃), 40.2 (CH₂); HRMS (ESI-MS) *m/z*: [M + H]⁺ calcd for C₁₉H₁₇ClO₃⁺: 329.0947; found: 329.0937; IR (cm⁻¹): 2937 (OCH₃), 1704 (C=O), 1165 (Ar-C=C), 741 (Cl).

4-allyl-2-methoxyphenyl (E)-3-(4-chlorophenyl)acrylate (c7). White solid; yield 62% (the crude was purified using a mixture of PE/EtOAc 100:1); mp: 282.3–283.3 °C; ¹H NMR (500 MHz, CDCl₃) δ 7.82 (d, *J* = 16.0 Hz, 1H, Ar-H), 7.52 (s, 1H, Ar-H), 7.50 (d, 1H, CH), 7.40 (s, 1H, Ar-H), 7.38 (s, 1H, Ar-H), 7.02 (d, *J* = 8.0 Hz, 1H, Ar-H), 6.82 (s, 1H, Ar-H), 6.80 (d, *J* = 8.0 Hz, 1H, Ar-H), 6.64 (d, *J* = 15.9 Hz, 1H, CH), 5.98 (td, *J* = 16.9, 6.7 Hz, 1H, CH), 5.17–5.09 (m, 2H, CH₂), 3.83 (s, 3H, OCH₃), 3.40 (d, *J* = 6.7 Hz, 2H, CH₂); ¹³C NMR (126 MHz, CDCl₃) δ 165.0 (C=O), 151.0 (Ar-C), 145.1 (CH), 139.2 (Ar-C), 137.2 (CH), 136.7 (Ar-C), 136.6 (Ar-C), 132.9 (Ar-C), 129.6 (Ar-2C), 129.4 (Ar-2C), 122.7 (Ar-C), 120.8 (Ar-C), 117.8 (CH), 116.3 (CH), 112.9 (Ar-C), 56.0 (OCH₃), 40.2 (CH₂); HRMS (ESI-MS) *m/z*: [M + H]⁺ calcd for C₁₉H₁₇ClO₃⁺: 329.0947; found: 329.0936; IR (cm⁻¹): 2937 (OCH₃), 1704 (C=O), 1165 (Ar-C=C), 755 (Cl).

4-allyl-2-methoxyphenyl (E)-3-(2-fluorophenyl)acrylate (c8). Yellow solid; yield 69% (the crude was purified using a mixture of PE/EtOAc 100:1); mp: 270.6–271.2 °C; ¹H NMR (500 MHz, CDCl₃) δ 8.00 (d, *J* = 16.2 Hz, 1H, Ar-H), 7.61 (t, *J* = 7.6 Hz, 1H, Ar-H), 7.39 (d, *J* = 8.2 Hz, 1H, CH), 7.20 (t, *J* = 7.5 Hz, 1H, Ar-H), 7.13 (d, *J* = 18.9 Hz, 1H, Ar-H), 7.04 (d, *J* = 8.0 Hz, 1H, Ar-H), 6.83 (s, 1H, Ar-H), 6.81 (d, *J* = 7.8 Hz, 1H, Ar-H), 6.77 (s, 1H, CH), 6.04–5.94 (m, 1H, CH), 5.16–5.08 (m, 2H, CH₂), 3.84 (s, 3H, OCH₃), 3.41 (d, *J* = 6.7 Hz, 2H, CH₂); ¹³C NMR (126 MHz, CDCl₃) δ 165.1 (C=O), 162.6 (Ar-C), 160.6 (Ar-C), 151.1 (CH), 139.1 (Ar-C), 138.1 (CH), 137.2 (Ar-C), 132.2 (Ar-C), 132.1 (Ar-C), 129.4 (Ar-C), 124.7 (Ar-C), 124.7 (Ar-C), 122.7 (Ar-C), 120.8 (CH), 119.8 (CH), 116.3 (Ar-C), 112.9 (Ar-C), 56.0 (OCH₃), 40.2 (CH₂); HRMS (ESI-MS) *m/z*: [M + H]⁺ calcd for C₁₉H₁₇FO₃⁺: 313.1243; found: 313.1231; IR (cm⁻¹): 2937 (-CH₃O), 1704 (C=O), 1165 (Ar-C=C), 1317 (F).

4-allyl-2-methoxyphenyl (E)-3-(3-fluorophenyl)acrylate (c9). Yellow solid; yield 45% (the crude was purified using a mixture of PE/EtOAc 100:1); mp: 279.6–280.4 °C; ¹H NMR (500 MHz, CDCl₃) δ 7.82 (d, *J* = 16.0 Hz, 1H, Ar-H), 7.39 (d, *J* = 5.5 Hz, 1H, Ar-H), 7.35 (d, *J* = 7.8 Hz, 1H, CH), 7.28 (d, *J* = 9.5 Hz, 1H, Ar-H), 7.12 (d, *J* = 9.3 Hz, 1H, Ar-H), 7.03 (d, *J* = 8.0 Hz, 1H, Ar-H), 6.83 (s, *J* = 1.9 Hz, 1H, Ar-H), 6.81 (d, *J* = 7.9 Hz, 1H, Ar-H), 6.66 (d, *J* = 16.0 Hz, 1H, CH), 5.98 (td, *J* = 16.8, 6.7 Hz, 1H, CH), 5.16–5.09 (m, 2H, CH₂), 3.83 (s, 3H, OCH₃), 3.40 (d, *J* = 6.8 Hz, 2H, CH₂); ¹³C NMR (126 MHz, CDCl₃) δ 164.9 (C=O),

164.1 (Ar-C), 162.2 (Ar-C), 151.1 (Ar-C), 145.1 (Ar-C), 139.3 (CH), 138.0 (Ar-C), 137.2 (CH), 130.7 (Ar-C), 124.4 (Ar-C), 122.7 (Ar-C), 120.9 (Ar-C), 118.7 (Ar-C), 117.6 (CH), 116.3 (CH), 114.7 (Ar-C), 112.9 (Ar-C), 56.0 (OCH₃), 40.2 (CH₂); HRMS (ESI-MS) m/z: [M + H]⁺ calcd for C₁₉H₁₇FO₃⁺: 313.1243; found: 313.1231; IR (cm⁻¹): 2937 (OCH₃), 1704 (C=O), 1165 (Ar-C=C), 1325 (F).

4-allyl-2-methoxyphenyl (E)-3-(4-fluorophenyl)acrylate (c10). Yellow solid; yield 50% (the crude was purified using a mixture of PE/EtOAc 100:1); mp: 270.4–270.6 °C; ¹H NMR (500 MHz, CDCl₃) δ 7.83 (d, J = 16.0 Hz, 1H, Ar-H), 7.58 (d, J = 5.4 Hz, 1H, Ar-H), 7.57 (d, J = 5.6 Hz, 1H, CH), 7.12 (s, 1H, Ar-H), 7.10 (d, J = 8.6 Hz, 1H, Ar-H), 7.03 (d, J = 8.0 Hz, 1H, Ar-H), 6.82 (s, 1H, Ar-H), 6.81 (d, J = 8.1 Hz, 1H, Ar-H), 6.60 (d, J = 16.0 Hz, 1H, CH), 5.98 (td, J = 16.8, 6.7 Hz, 1H, CH), 5.16–5.09 (m, 2H, CH₂), 3.83 (s, 3H, OCH₃), 3.40 (d, J = 6.7 Hz, 2H, CH₂); ¹³C NMR (126 MHz, CDCl₃) δ 165.1 (C=O), 163.2 (Ar-C), 151.1 (Ar-C), 145.2 (CH), 139.2 (Ar-C), 138.0 (Ar-C), 137.2 (CH), 130.7 (Ar-C), 130.4 (Ar-C), 130.3 (Ar-C), 122.7 (Ar-C), 120.8 (Ar-C), 117.0 (CH), 116.4 (CH), 116.3 (Ar-C), 116.2 (Ar-C), 112.9 (Ar-C), 56.0 (OCH₃), 40.3 (CH₂). HRMS (ESI-MS) m/z: [M + H]⁺ calcd for C₁₉H₁₇FO₃⁺: 313.1243; found: 313.1231; IR (cm⁻¹): 2937 (OCH₃), 1704 (C=O), 1165 (Ar-C=C), 1323 (F).

4-allyl-2-methoxyphenyl (E)-3-(2-bromophenyl)acrylate (c11). Yellow solid; yield 54% (the crude was purified using a mixture of PE/EtOAc 100:1); mp: 296.3–296.5 °C; ¹H NMR (500 MHz, CDCl₃) δ 8.25 (d, J = 15.9 Hz, 1H, Ar-H), 7.70 (d, J = 7.9 Hz, 1H, Ar-H), 7.64 (d, J = 8.1 Hz, 1H, CH), 7.36 (t, J = 7.6 Hz, 1H, Ar-H), 7.26 (d, J = 8.0 Hz, 1H, Ar-H), 7.05 (d, J = 8.0 Hz, 1H, Ar-H), 6.83 (s, 1H, Ar-H), 6.81 (d, J = 7.9 Hz, 1H, Ar-H), 6.63 (d, J = 16.0 Hz, 1H, CH), 6.04 (td, J = 16.8, 6.7 Hz, 1H, CH), 5.16–5.09 (m, 2H, CH₂), 3.84 (s, 3H, OCH₃), 3.41 (d, J = 6.8 Hz, 2H, CH₂); ¹³C NMR (126 MHz, CDCl₃) δ 164.7 (C=O), 151.1 (Ar-C), 144.8 (CH), 139.2 (Ar-C), 138.0 (CH), 137.2 (Ar-C), 134.5 (Ar-C), 133.7 (Ar-C), 131.6 (Ar-C), 128.0 (Ar-C), 127.9 (Ar-C), 125.7 (Ar-C), 122.7 (Ar-C), 120.8 (Ar-C), 120.0 (CH), 116.1 (CH), 112.9 (Ar-C), 56.0 (OCH₃), 40.2 (CH₂); HRMS (ESI-MS) m/z: [M + H]⁺ calcd for C₁₉H₁₇BrO₃⁺: 373.0442; found: 373.0430 IR (cm⁻¹): 2937 (OCH₃), 1704 (C=O), 1165 (Ar-C=C), 568 (Br).

4-allyl-2-methoxyphenyl (E)-3-(3-bromophenyl)acrylate (c12). White solid; yield 61% (the crude was purified using a mixture of PE/EtOAc 100:1); mp: 272.6–272.8 °C; ¹H NMR (500 MHz, CDCl₃) δ 7.78 (d, J = 16.0 Hz, 1H, Ar-H), 7.73 (s, 1H, Ar-H), 7.54 (d, J = 7.9 Hz, 1H, CH), 7.50 (d, J = 7.8 Hz, 1H, Ar-H), 7.29 (t, J = 7.9 Hz, 1H, Ar-H), 7.02 (d, J = 7.9 Hz, 1H, Ar-H), 6.82 (s, 1H, Ar-H), 6.80 (d, J = 8.0 Hz, 1H, Ar-H), 6.66 (d, J = 16.0 Hz, 1H, CH), 5.98 (td, J = 16.8, 6.8 Hz, 1H, CH), 5.16–5.09 (m, 2H, CH₂), 3.83 (s, 3H, OCH₃), 3.40 (d, J = 6.7 Hz, 2H, CH₂); ¹³C NMR (126 MHz, CDCl₃) δ 164.8 (C=O), 151.0 (Ar-C), 144.8 (CH), 139.2 (Ar-C), 138.0 (Ar-C), 137.2 (CH₂), 136.5 (Ar-C), 133.5 (Ar-C), 131.1 (Ar-C), 130.6 (Ar-C), 127.0 (Ar-C), 123.2 (Ar-C), 122.7 (Ar-C), 120.9 (CH), 118.8 (CH), 116.3 (Ar-C), 112.9 (Ar-C), 56.0 (OCH₃), 40.3 (CH); HRMS (ESI-MS) m/z: [M + H]⁺ calcd for C₁₉H₁₇BrO₃⁺: 373.0442; found: 313.0433; IR (cm⁻¹): 2937 (OCH₃), 1704 (C=O), 1165 (Ar-C=C), 559 (Br).

4-allyl-2-methoxyphenyl (E)-3-(4-bromophenyl)acrylate (c13). White solid; yield 58% (the crude was purified using a mixture of PE/EtOAc 100:1); mp: 239.9–340.9 °C; ¹H NMR (500 MHz, CDCl₃) δ 7.80 (d, J = 16.1 Hz, 1H, Ar-H), 7.56 (s, 1H, Ar-H), 7.54 (s, 1H, CH), 7.45 (s, 1H, Ar-H), 7.43 (s, 1H, Ar-H), 7.02 (d, J = 7.9 Hz, 1H, Ar-H), 6.82 (s, 1H, Ar-H), 6.80 (d, J = 8.0 Hz, 1H, Ar-H), 6.66 (d, J = 16.0 Hz, 1H, CH), 5.98 (td, J = 16.9, 6.7 Hz, 1H, CH), 5.15–5.09 (m, 2H, CH₂), 3.83 (s, 3H, OCH₃), 3.40 (d, J = 6.7 Hz, 2H, CH₂); ¹³C NMR (126 MHz, CDCl₃) δ 165.3 (C=O), 151.3 (Ar-C), 145.4 (CH), 139.5 (Ar-C), 138.2 (Ar-C), 137.4 (CH), 133.6 (Ar-C), 132.6 (Ar-2C), 130.0 (Ar-2C), 125.3 (Ar-C), 123.0 (Ar-C), 121.1 (CH), 118.2 (CH), 116.6 (Ar-C), 113.1 (Ar-C), 56.3 (OCH₃), 40.5 (CH₂); HRMS (ESI-MS) m/z: [M + H]⁺ calcd for C₁₉H₁₇BrO₃⁺: 373.0442; found: 373.0429; IR (cm⁻¹): 2937 (OCH₃), 1704 (C=O), 1165 (Ar-C=C), 571 (Br).

4-allyl-2-methoxyphenyl (E)-3-(3-hydroxyphenyl)acrylate (c14). White solid; yield 51% (the crude was purified using a mixture of PE/EtOAc 40:1); mp: 322.2–322.4 °C; ¹H NMR (500 MHz, CDCl₃) δ 7.80 (d, J = 15.9 Hz, 1H, Ar-H), 7.25 (t, J = 7.9 Hz, 1H, Ar-H), 7.12 (d, J = 7.9 Hz, 1H, CH), 7.03 (d, J = 7.9 Hz, 1H, Ar-H), 7.00 (t, J = 2.1 Hz, 1H, Ar-H), 6.86 (d, J = 8.1 Hz, 1H, Ar-H), 6.82 (s, 1H, Ar-H), 6.81–6.78 (m, 1H, Ar-H), 6.61 (d, J = 15.9

Hz, 1H, CH), 6.01–5.92 (m, 1H, CH), 5.14–5.08 (m, 2H, CH₂), 3.82 (s, 3H, OCH₃), 3.38 (d, $J = 6.7$ Hz, 2H, CH₂); ¹³C NMR (126 MHz, CDCl₃) δ 165.7 (C=O), 156.3 (Ar-C), 151.0 (Ar-C), 146.7 (Ar-C), 139.3 (CH), 138.0 (Ar-C), 137.2 (CH), 135.8 (Ar-C), 130.2 (Ar-C), 122.7 (Ar-C), 121.0 (Ar-C), 120.9 (Ar-C), 118.0 (Ar-C), 117.3 (CH), 116.3 (CH), 114.8 (Ar-C), 112.9 (Ar-C), 56.0 (OCH₃), 40.2 (CH₂); HRMS (ESI-MS) m/z : [M + H]⁺ calcd for C₁₉H₁₈O₄⁺: 311.1286; found: 311.1275; IR (cm⁻¹): 3376 (OH), 2937 (OCH₃), 1704 (C=O), 1165 (Ar-C=C).

4-allyl-2-methoxyphenyl (E)-3-(4-hydroxyphenyl)acrylate (c15). White solid; yield 47% (the crude was purified using a mixture of PE/EtOAc 40:1); mp: 296.3–296.5 °C; ¹H NMR (500 MHz, CDCl₃) δ 7.81 (d, $J = 15.9$ Hz, 1H, Ar-H), 7.46 (d, 1H, Ar-H), 7.45 (d, 1H, CH), 7.03 (d, $J = 7.9$ Hz, 1H, Ar-H), 6.84 (d, 1H, Ar-H), 6.82–6.81 (m, 1H, Ar-H), 6.79 (s, 1H, Ar-H), 6.51 (d, $J = 15.9$ Hz, 1H, Ar-H), 5.97 (td, $J = 16.8, 6.7$ Hz, 1H, CH), 5.83 (s, 1H, CH), 5.15–5.07 (m, 2H, CH₂), 3.82 (s, 3H, OCH₃), 3.39 (d, $J = 6.7$ Hz, 2H, CH₂); ¹³C NMR (126 MHz, CDCl₃) δ 166.0 (C=O), 158.3 (Ar-C), 151.1 (Ar-C), 146.6 (CH), 139.2 (Ar-C), 138.0 (CH), 137.2 (Ar-C), 130.4 (Ar-2C), 127.0 (Ar-C), 122.8 (Ar-C), 120.9 (Ar-C), 116.3 (CH), 116.1 (Ar-2C), 114.3 (CH), 112.9 (Ar-C), 56.0 (OCH₃), 40.3 (CH₂); HRMS (ESI-MS) m/z : [M + H]⁺ calcd for C₁₉H₁₈O₄⁺: 311.1286; found: 311.1273; IR (cm⁻¹): 3371 (OH), 2937 (OCH₃), 1704 (C=O), 1165 (Ar-C=C).

4-allyl-2-methoxyphenyl (E)-3-(2-nitrophenyl)acrylate (c16). Yellow solid; yield 42% (the crude was purified using a mixture of PE/EtOAc 100:1); mp: 295.2–295.4 °C; ¹H NMR (500 MHz, CDCl₃) δ 8.31 (d, $J = 15.8$ Hz, 1H, Ar-H), 8.07 (d, $J = 8.1$ Hz, 1H, Ar-H), 7.73 (d, $J = 6.2$ Hz, 1H, CH), 7.69 (t, $J = 7.6$ Hz, 1H, Ar-H), 7.58 (t, $J = 7.8$ Hz, 1H, Ar-H), 7.04 (d, $J = 7.9$ Hz, 1H, Ar-H), 6.84–6.82 (m, 1H, Ar-H), 6.81 (d, $J = 8.0$ Hz, 1H, Ar-H), 6.59 (d, $J = 15.8$ Hz, 1H, CH), 5.98 (td, $J = 16.9, 6.7$ Hz, 1H, CH), 5.14–5.09 (m, 2H, CH₂), 3.84 (s, 3H, OCH₃), 3.40 (d, $J = 6.5$ Hz, 2H, CH₂); ¹³C NMR (126 MHz, CDCl₃) δ 164.1 (C=O), 151.0 (Ar-C), 148.5 (Ar-C), 141.7 (CH), 139.3 (Ar-C), 138.0 (Ar-C), 137.2 (CH), 133.8 (Ar-C), 130.7 (Ar-C), 130.6 (Ar-C), 129.4 (Ar-C), 125.1 (Ar-C), 122.7 (Ar-C), 122.4 (Ar-C), 120.8 (CH), 116.3 (CH), 112.9 (Ar-C), 56.0 (OCH₃), 40.3 (CH₂); HRMS (ESI-MS) m/z : [M + H]⁺ calcd for C₁₉H₁₇NO₅⁺: 340.1181; found: 340.1176; IR (cm⁻¹): 2937 (OCH₃), 1704 (C=O), 1424 (NO₂), 1165 (Ar-C=C).

4-allyl-2-methoxyphenyl (E)-3-(3-nitrophenyl)acrylate (c17). White solid; yield 51% (the crude was purified using a mixture of PE/EtOAc 100:1); mp: 255.5–256.1 °C; ¹H NMR (500 MHz, CDCl₃) δ 8.44 (t, $J = 1.9$ Hz, 1H, Ar-H), 8.26 (d, $J = 9.9$ Hz, 1H, Ar-H), 7.90 (d, $J = 11.4$ Hz, 1H, CH), 7.88 (d, $J = 3.2$ Hz, 1H, Ar-H), 7.61 (t, $J = 8.0$ Hz, 1H, Ar-H), 7.03 (d, $J = 8.0$ Hz, 1H, Ar-H), 6.83 (d, $J = 1.9$ Hz, 1H, Ar-H), 6.81 (d, $J = 2.8$ Hz, 1H, Ar-H), 6.79 (d, $J = 11.1$ Hz, 1H, CH), 5.98 (td, $J = 16.9, 6.7$ Hz, 1H, CH), 5.16–5.08 (m, 2H, CH₂), 3.83 (s, 3H, OCH₃), 3.40 (d, $J = 6.7$ Hz, 2H, CH₂); ¹³C NMR (126 MHz, CDCl₃) δ 164.4 (C=O), 151.7 (Ar-C), 148.8 (Ar-C), 143.5 (CH), 139.4 (Ar-C), 137.9 (Ar-C), 137.1 (CH), 136.1 (Ar-C), 133.9 (Ar-C), 130.2 (Ar-C), 124.9 (Ar-C), 122.8 (Ar-C), 122.6 (Ar-C), 120.8 (Ar-C), 120.5 (CH), 116.4 (CH), 112.9 (Ar-C), 56.0 (OCH₃), 40.3 (CH₂); HRMS (ESI-MS) m/z : [M + H]⁺ calcd for C₁₉H₁₇NO₅⁺: 340.1181; found: 340.1178; IR (cm⁻¹): 2937 (OCH₃), 1704 (C=O), 1421 (NO₂), 1165 (Ar-C=C).

4-allyl-2-methoxyphenyl (E)-3-(4-nitrophenyl)acrylate (c18). Yellow solid; yield 58% (the crude was purified using a mixture of PE/EtOAc 80:1); mp: 291.2–292.3 °C; ¹H NMR (500 MHz, CDCl₃) δ 8.28 (d, $J = 1.8$ Hz, 1H, Ar-H), 8.27 (d, $J = 2.0$ Hz, 1H, Ar-H), 7.89 (d, $J = 16.0$ Hz, 1H, CH), 7.74 (d, $J = 2.0$ Hz, 1H, Ar-H), 7.72 (d, $J = 2.1$ Hz, 1H, Ar-H), 7.03 (d, $J = 8.0$ Hz, 1H, Ar-H), 6.83 (d, $J = 1.3$ Hz, 1H, Ar-H), 6.81 (d, $J = 5.7$ Hz, 1H, Ar-H), 6.79 (d, $J = 13.7$ Hz, 1H, CH), 5.97 (td, $J = 16.8, 6.7$ Hz, 1H, CH), 5.16–5.09 (m, 2H, CH₂), 3.83 (s, 3H, OCH₃), 3.40 (d, $J = 6.7$ Hz, 2H, CH₂); ¹³C NMR (126 MHz, CDCl₃) δ 164.3 (C=O), 151.0 (Ar-C), 148.8 (CH), 143.5 (Ar-C), 140.5 (CH), 139.5 (Ar-C), 137.8 (Ar-C), 137.0 (Ar-C), 129.0 (Ar-2C), 124.4 (Ar-2C), 122.6 (Ar-C), 121.6 (Ar-C), 120.9 (CH), 116.4 (CH), 112.8 (Ar-C), 56.0 (OCH₃), 40.3 (CH₂); HRMS (ESI-MS) m/z : [M + H]⁺ calcd for C₁₉H₁₇NO₅⁺: 340.1181; found: 340.1178; IR (cm⁻¹): 2937 (OCH₃), 1704 (C=O), 1424 (NO₂), 1165 (Ar-C=C).

4-allyl-2-methoxyphenyl (E)-3-(2-methoxyphenyl)acrylate (c19). White solid; yield 49% (the crude was purified using a mixture of PE/EtOAc 80:1); mp: 250.3–250.8 °C; ¹H

NMR (500 MHz, CDCl₃) δ 8.17 (d, J = 16.1 Hz, 1H, Ar-H), 7.57 (d, J = 7.7 Hz, 1H, Ar-H), 7.38 (t, J = 8.7 Hz, 1H, CH), 7.03 (d, J = 7.9 Hz, 1H, Ar-H), 6.99 (t, J = 7.5 Hz, 1H, Ar-H), 6.94 (d, J = 8.3 Hz, 1H, Ar-H), 6.82 (d, J = 1.9 Hz, 1H, Ar-H), 6.81 (s, 1H, Ar-H), 6.78 (d, J = 9.2 Hz, 1H, CH), 5.99 (td, J = 16.8, 6.7 Hz, 1H, CH), 5.16–5.08 (m, 2H, CH₂), 3.90 (s, 3H, CH₃), 3.83 (s, 3H, OCH₃), 3.40 (d, J = 6.7 Hz, 2H, CH₂); ¹³C NMR (126 MHz, CDCl₃) δ 165.8 (C=O), 158.7 (Ar-C), 151.2 (Ar-C), 142.1 (CH), 139.0 (Ar-C), 138.2 (CH), 137.3 (Ar-C), 131.9 (Ar-C), 129.5 (Ar-C), 123.4 (Ar-C), 122.8 (Ar-C), 120.9 (Ar-C), 120.8 (Ar-C), 117.7 (CH), 116.3 (CH), 112.9 (Ar-C), 111.3 (Ar-C), 56.0 (OCH₃), 55.6 (OCH₃), 40.3 (CH₂); HRMS (ESI-MS) m/z : [M + H]⁺ calcd for C₂₀H₂₀O₄⁺: 325.1437; found: 325.1432; IR (cm⁻¹): 2937, 2873 (OCH₃), 1704 (C=O), 1165 (Ar-C=C).

4-allyl-2-methoxyphenyl (E)-3-(3-methoxyphenyl)acrylate (c20). White solid; yield 60% (the crude was purified using a mixture of PE/EtOAc 100:1); mp: 246.3–246.4 °C; ¹H NMR (500 MHz, CDCl₃) δ 7.84 (d, J = 16.0 Hz, 1H, Ar-H), 7.33 (t, J = 7.9 Hz, 1H, Ar-H), 7.18 (d, J = 7.8 Hz, 1H, CH), 7.11 (t, J = 2.1 Hz, 1H, Ar-H), 7.03 (d, J = 8.0 Hz, 1H, Ar-H), 6.97 (d, J = 8.6 Hz, 1H, Ar-H), 6.83 (d, J = 1.9 Hz, 1H, Ar-H), 6.81 (d, J = 8.0 Hz, 1H, Ar-H), 6.67 (d, J = 15.9 Hz, 1H, CH), 5.98 (td, J = 16.9, 6.8 Hz, 1H, CH), 5.16–5.09 (m, 2H, CH₂), 3.85 (s, 3H, OCH₃), 3.83 (s, 3H, CH₃), 3.40 (d, J = 6.7 Hz, 2H, CH₂); ¹³C NMR (126 MHz, CDCl₃) δ 165.2 (C=O), 160.0 (Ar-C), 151.1 (Ar-C), 146.5 (CH), 139.1 (Ar-C), 138.1 (CH), 137.2 (Ar-C), 135.8 (Ar-C), 130.1 (Ar-C), 122.8 (Ar-C), 121.2 (Ar-C), 120.9 (Ar-C), 117.5 (Ar-C), 116.7 (CH), 116.3 (CH), 113.1 (Ar-C), 112.9 (Ar-C), 56.0 (OCH₃), 55.4 (OCH₃), 40.2 (CH₂); HRMS (ESI-MS) m/z : [M + H]⁺ calcd for C₂₀H₂₀O₄⁺: 325.1437; found: 325.1432; IR (cm⁻¹): 2937, 2867 (OCH₃), 1704 (CO), 1165 (PH-C=C).

4-allyl-2-methoxyphenyl (E)-3-(4-methoxyphenyl)acrylate (c21). White solid; yield 62% (the crude was purified using a mixture of PE/EtOAc 100:1); mp: 328.6–329.0 °C; ¹H NMR (500 MHz, CDCl₃) δ 7.83 (d, J = 15.9 Hz, 1H, Ar-H), 7.55 (s, 1H, Ar-H), 7.53 (d, 1H, CH), 7.03 (d, J = 7.9 Hz, 1H, Ar-H), 6.94 (d, J = 2.1 Hz, 1H, Ar-H), 6.93 (d, J = 2.0 Hz, 1H, Ar-H), 6.82 (d, J = 1.9 Hz, 1H, Ar-H), 6.80 (d, J = 7.9 Hz, 1H, Ar-H), 6.54 (d, J = 15.9 Hz, 1H, CH), 5.98 (td, J = 16.9, 6.7 Hz, 1H, CH), 5.17–5.08 (m, 2H, CH₂), 3.85 (s, 3H, CH₃), 3.83 (s, 3H, OCH₃), 3.40 (d, J = 6.8 Hz, 2H, CH₂); ¹³C NMR (126 MHz, CDCl₃) δ 165.6 (C=O), 161.7 (Ar-C), 151.2 (Ar-C), 146.3 (CH), 139.0 (Ar-C), 138.2 (CH), 137.2 (Ar-C), 130.1 (Ar-2C), 127.2 (Ar-C), 122.9 (Ar-C), 120.9 (Ar-C), 116.3 (CH), 114.6 (CH), 114.5 (Ar-2C), 112.8 (Ar-C), 56.0 (OCH₃), 55.5 (OCH₃), 40.2 (CH₂); HRMS (ESI-MS) m/z : [M + H]⁺ calcd for C₂₀H₂₀O₄⁺: 325.1437; found: 325.1432; IR (cm⁻¹): 2937, 2871 (OCH₃), 1704 (C=O), 1165 (Ar-C=C).

4-allyl-2-methoxyphenyl (E)-3-(2-(trifluoromethyl)phenyl)acrylate (c22). White solid; yield 47% (the crude was purified using a mixture of PE/EtOAc 100:1); mp: 339.4–340.1 °C; ¹H NMR (500 MHz, CDCl₃) δ 8.25 (d, J = 15.8 Hz, 1H, Ar-H), 7.80 (d, J = 7.8 Hz, 1H, Ar-H), 7.73 (d, J = 7.9 Hz, 1H, CH), 7.61 (t, J = 7.7 Hz, 1H, Ar-H), 7.54–7.49 (m, 1H, Ar-H), 7.05 (d, J = 7.9 Hz, 1H, Ar-H), 6.83 (d, J = 1.9 Hz, 1H, Ar-H), 6.81 (d, J = 8.0 Hz, 1H, Ar-H), 6.65 (d, J = 15.8 Hz, 1H, CH), 5.98 (td, J = 16.8, 6.7 Hz, 1H, CH), 5.16–5.09 (m, 2H, CH₂), 3.84 (s, 3H, OCH₃), 3.41 (d, J = 6.8 Hz, 2H, CH₂); ¹³C NMR (126 MHz, CDCl₃) δ 164.4 (C=O), 151.1 (Ar-C), 141.9 (Ar-C), 139.2 (CH), 138.0 (Ar-C), 137.2 (CH), 133.3 (Ar-C), 132.3 (Ar-C), 130.0 (Ar-C), 129.3 (Ar-C), 128.2 (Ar-C), 126.4 (Ar-C), 125.1 (Ar-C), 122.7 (Ar-C), 121.6 (CF₃), 120.9 (CH), 116.3 (CH), 113.9 (Ar-C), 56.0 (OCH₃), 40.3 (CH₂); HRMS (ESI-MS) m/z : [M + H]⁺ calcd for C₂₀H₁₇F₃O₃⁺: 363.1205; found: 363.1198; IR (cm⁻¹): 2937 (OCH₃), 1704 (C=O), 1332 (CF₃), 1165 (Ar-C=C).

4-allyl-2-methoxyphenyl (E)-3-(3-(trifluoromethyl)phenyl)acrylate (c23). Yellow solid; yield 69% (the crude was purified using a mixture of PE/EtOAc 100:1); mp: 339.1–339.3 °C; ¹H NMR (500 MHz, CDCl₃) δ 7.88 (d, J = 16.0 Hz, 1H, Ar-H), 7.83 (s, 1H, Ar-H), 7.76 (d, J = 7.8 Hz, 1H, CH), 7.67 (d, J = 7.1 Hz, 1H, Ar-H), 7.55 (t, J = 7.8 Hz, 1H, Ar-H), 7.03 (d, J = 8.0 Hz, 1H, Ar-H), 6.83 (d, J = 2.0 Hz, 1H, Ar-H), 6.81 (dd, J = 8.0, 1.9 Hz, 1H, Ar-H), 6.74 (d, J = 16.0 Hz, 1H, CH), 5.98 (td, J = 16.9, 6.7 Hz, 1H, CH), 5.16–5.09 (m, 2H, CH₂), 3.83 (s, 3H, OCH₃), 3.40 (d, J = 6.7 Hz, 2H, CH₂); ¹³C NMR (126 MHz, CDCl₃) δ 164.7 (C=O), 151.0 (Ar-C), 144.7 (CH), 139.3 (Ar-C), 138.0 (CH), 137.2 (Ar-C), 135.2 (Ar-C), 131.8 (Ar-C), 131.4 (Ar-C), 129.7 (Ar-C), 127.1 (CF₃), 125.0 (Ar-C), 122.7 (Ar-C), 120.9 (Ar-C), 119.3 (Ar-C), 116.4

(CH), 112.9 (CH), 56.0 (Ar-C), 55.9 (OCH₃), 40.3 (CH₂); HRMS (ESI-MS) *m/z*: [M + H]⁺ calcd for C₂₀H₁₇F₃O₃⁺: 363.1205; found: 363.1199; IR (cm⁻¹): 2937 (OCH₃), 1704 (C=O), 1330 (CF₃), 1165 (Ar-C=C).

4-allyl-2-methoxyphenyl (E)-3-(4-(trifluoromethyl)phenyl)acrylate (c24). White soild; yield 42% (the crude was purified using a mixture of PE/EtOAc 60:1); mp: 343.2–343.3 °C; ¹H NMR (500 MHz, CDCl₃) δ 7.88 (d, *J* = 16.0 Hz, 1H, Ar-H), 7.68 (s, 1H, Ar-H), 7.68 (s, 1H, CH), 7.68 (s, 1H, Ar-H), 7.68 (s, 1H, Ar-H), 7.03 (d, *J* = 7.9 Hz, 1H, Ar-H), 6.83 (d, *J* = 1.9 Hz, 1H, Ar-H), 6.81 (dd, *J* = 8.0, 1.9 Hz, 1H, Ar-H), 6.75 (d, *J* = 16.0 Hz, 1H, CH), 5.98 (td, *J* = 16.8, 6.7 Hz, 1H, CH), 5.16–5.06 (m, 2H, CH₂), 3.83 (s, 3H, OCH₃), 3.41 (d, *J* = 6.7 Hz, 2H, CH₂); ¹³C NMR (126 MHz, CDCl₃) δ 164.7 (C=O), 151.0 (Ar-C), 144.6 (CH), 139.4 (Ar-C), 137.0 (Ar-C), 137.8 (CH), 137.1 (Ar-C), 132.0 (Ar-C), 128.5 (Ar-2C), 126.1 (Ar-2C), 126.0 (CF₃), 122.7 (Ar-C), 120.9 (Ar-C), 119.9 (CH), 116.4 (CH), 112.9 (Ar-C), 56.0 (OCH₃), 40.3 (CH₂); HRMS (ESI-MS) *m/z*: [M + H]⁺ calcd for C₂₀H₁₇F₃O₃⁺: 363.1205; found: 363.1200; IR (cm⁻¹): 2937 (OCH₃), 1704 (C=O), 1331 (CF₃), 1165 (Ar-C=C).

4-allyl-2-methoxyphenyl (E)-3-(4-(dimethylamino)phenyl)acrylate (c25). Yellow soild; yield 29% (the crude was purified using a mixture of PE/EtOAc 40:1); mp: 328.6–329.1 °C; ¹H NMR (500 MHz, CDCl₃) δ 7.80 (d, *J* = 15.8 Hz, 1H, Ar-H), 7.49 (s, 1H, Ar-H), 7.47 (s, 1H, CH), 7.02 (d, *J* = 7.9 Hz, 1H, Ar-H), 6.81 (d, *J* = 1.9 Hz, 1H, Ar-H), 6.79 (dd, *J* = 7.9, 1.9 Hz, 1H, Ar-H), 6.70 (s, 1H, Ar-H), 6.68 (d, 1H, Ar-H), 6.44 (d, *J* = 15.8 Hz, 1H, CH), 5.98 (td, *J* = 16.8, 6.7 Hz, 1H, CH), 5.17–5.07 (m, 2H, CH₂), 3.83 (s, 3H, OCH₃), 3.39 (d, *J* = 6.8 Hz, 2H, CH₂), 3.04 (s, 6H, CH₃, CH₃); ¹³C NMR (126 MHz, CDCl₃) δ 166.2 (C=O), 152.0 (CH), 151.3 (Ar-C), 147.2 (Ar-C), 138.8 (CH), 138.4 (Ar-C), 137.3 (Ar-C), 130.2 (Ar-C), 123.0 (Ar-C), 120.8 (Ar-C), 116.2 (CH), 112.8 (CH), 112.0 (Ar-C), 111.3 (Ar-C), 56.0 (OCH₃), 40.3 ((CH₃)₂), 40.3 (CH₂); HRMS (ESI-MS) *m/z*: [M + H]⁺ calcd for C₂₁H₂₃NO₃⁺: 338.1754; found: 338.1746; IR (cm⁻¹): 2937 (OCH₃), 2925 (CH₂), 2968 (CH₃), 1704 (C=O), 1609 (N), 1165 (Ar-C=C).

4-allyl-2-methoxyphenyl (E)-3-(4-hydroxy-3-methoxyphenyl)acrylate (c26). White soild; yield 56% (the crude was purified using a mixture of PE/EtOAc 100:1); mp: 274.3–274.8 °C; ¹H NMR (500 MHz, CDCl₃) δ 7.80 (d, *J* = 15.9 Hz, 1H, Ar-H), 7.13 (d, *J* = 8.1 Hz, 1H, Ar-H), 7.10 (d, *J* = 1.9 Hz, 1H, CH), 7.02 (d, *J* = 7.9 Hz, 1H, Ar-H), 6.94 (d, *J* = 8.2 Hz, 1H, Ar-H), 6.82 (d, *J* = 1.9 Hz, 1H, Ar-H), 6.80 (d, *J* = 8.0 Hz, 1H, Ar-H), 6.52 (d, *J* = 15.9 Hz, 1H, CH), 5.99 (dd, *J* = 16.9, 6.8 Hz, 1H, CH), 5.95–5.87 (m, 1H, CH), 5.16–5.08 (m, 2H, CH₂), 3.93 (s, 3H, CH₃), 3.83 (s, 3H, OCH₃), 3.40 (d, *J* = 6.8 Hz, 2H, CH₂); ¹³C NMR (126 MHz, CDCl₃) δ 165.6 (C=O), 151.2 (Ar-C), 148.4 (Ar-C), 146.9 (Ar-C), 146.7 (CH), 139.0 (Ar-C), 138.2 (CH), 137.2 (Ar-C), 127.0 (Ar-C), 123.6 (Ar-C), 122.8 (Ar-C), 120.8 (Ar-C), 116.3 (Ar-C), 114.9 (CH), 114.5 (CH), 112.9 (Ar-C), 109.5 (Ar-C), 56.1 (OCH₃), 56.00 (OCH₃), 40.3 (CH₂); HRMS (ESI-MS) *m/z*: [M + H]⁺ calcd for C₂₀H₂₀O₅⁺: 341.1386; found: 341.1380; IR (cm⁻¹): 3239 (OH), 2937, 2854 (OCH₃), 1704 (C=O), 1165 (Ar-C=C).

4-allyl-2-methoxyphenyl (E)-3-(3,4-dihydroxyphenyl)acrylate (c27). Yellow soild; yield 37% (the crude was purified using a mixture of PE/EtOAc 100:1); mp: 265.5–266.5 °C; ¹H NMR (500 MHz, CDCl₃) δ 7.72 (d, *J* = 15.8 Hz, 1H, Ar-H), 7.04 (s, 1H, Ar-H), 7.00 (d, *J* = 8.1 Hz, 1H, CH), 6.98 (d, *J* = 7.4 Hz, 1H, Ar-H), 6.82 (s, 1H, Ar-H), 6.79 (d, 1H, Ar-H), 6.77 (d, *J* = 2.0 Hz, 1H, Ar-H), 6.42 (d, *J* = 15.9 Hz, 1H, CH), 5.98–5.91 (m, 1H, CH), 5.14–5.07 (m, 2H, CH₂), 3.79 (s, 3H, OCH₃), 3.37 (d, *J* = 6.7 Hz, 2H, CH₂); ¹³C NMR (126 MHz, CDCl₃) δ 166.1 (C=O), 150.8 (Ar-C), 146.9 (CH), 146.8 (Ar-C), 143.9 (Ar-C), 139.0 (Ar-C), 137.8 (CH), 136.9 (Ar-C), 127.0 (Ar-C), 122.7 (Ar-C), 122.5 (Ar-C), 120.7 (Ar-C), 116.1 (Ar-C), 115.3 (CH), 114.4 (CH), 114.0 (Ar-C), 112.7 (Ar-C), 55.8 (OCH₃), 40.0 (CH₂); HRMS (ESI-MS) *m/z*: [M + H]⁺ calcd for C₁₉H₁₈O₅⁺: 327.1236; found: 327.1225; IR (cm⁻¹): 3217, 3186 (OH), 2937 (OCH₃), 1704 (C=O), 1165 (Ar-C=C).

4-allyl-2-methoxyphenyl (E)-3-(4-chloro-3-fluorophenyl)acrylate (c28). Yellow soild; yield 40% (the crude was purified using a mixture of PE/EtOAc 80:1); mp: 264.2–264.9 °C; ¹H NMR (500 MHz, CDCl₃) δ 7.76 (d, *J* = 16.0 Hz, 1H, Ar-H), 7.63 (dd, *J* = 7.0, 2.2 Hz, 1H, Ar-H), 7.45 (ddd, *J* = 8.6, 4.5, 2.2 Hz, 1H, CH), 7.19 (t, *J* = 8.6 Hz, 1H, Ar-H), 7.02 (d, *J* = 8.0 Hz, 1H, Ar-H), 6.82 (d, *J* = 2.0 Hz, 1H, Ar-H), 6.80 (d, *J* = 8.0 Hz, 1H, Ar-H), 6.60 (d, *J* = 16.0 Hz, 1H, CH), 5.98 (td, *J* = 16.8, 6.7 Hz, 1H, CH), 5.16–5.09 (m, 2H, CH₂), 3.83

(s, 3H, OCH₃), 3.40 (d, *J* = 6.8 Hz, 2H, CH₂); ¹³C NMR (126 MHz, CDCl₃) δ 164.7 (C=O), 160.4 (Ar-C), 158.3 (Ar-C), 151.0 (CH), 143.8 (Ar-C), 139.2 (CH), 137.9 (Ar-C), 137.2 (Ar-C), 131.8 (Ar-C), 130.4 (Ar-C), 128.3 (Ar-C), 122.7 (Ar-C), 120.9 (Ar-C), 118.4 (CH), 117.4 (CH), 116.3 (Ar-C), 112.8 (Ar-C), 56.0 (OCH₃), 40.3 (CH₂); HRMS (ESI-MS) *m/z*: [M + H]⁺ calcd for C₁₉H₁₆ClFO₃⁺: 347.0853; found: 347.0841; IR (cm⁻¹): 2937 (OCH₃), 1704 (C=O), 1165 (Ar-C=C), 1046 (F), 728 (Cl).

4-allyl-2-methoxyphenyl (E)-3-(benzo[d][1,3]dioxol-5-yl)acrylate (c29). White solid; yield 55% (the crude was purified using a mixture of PE/EtOAc 100:1); mp: 267.2–268.1 °C; ¹H NMR (500 MHz, CDCl₃) δ 7.77 (d, *J* = 15.9 Hz, 1H, CH), 7.09 (d, *J* = 1.7 Hz, 1H, Ar-H), 7.06 (d, *J* = 8.1 Hz, 1H, Ar-H), 7.02 (d, *J* = 8.0 Hz, 1H, Ar-H), 6.84 (d, *J* = 8.0 Hz, 1H, Ar-H), 6.82 (d, *J* = 1.9 Hz, 1H, Ar-H), 6.80 (d, *J* = 7.9 Hz, 1H, Ar-H), 6.49 (d, *J* = 15.9 Hz, 1H, CH), 6.02 (s, 2H, CH₂), 6.01–5.90 (m, 1H, CH), 5.15–5.06 (m, 2H, CH₂), 3.83 (s, 3H, OCH₃), 3.40 (d, *J* = 6.7 Hz, 2H, CH₂); ¹³C NMR (126 MHz, CDCl₃) δ 165.5 (C=O), 151.2 (Ar-C), 150.0 (Ar-C), 148.5 (Ar-C), 146.3 (Ar-C), 139.1 (CH), 138.1 (Ar-C), 137.2 (CH), 128.9 (Ar-C), 125.0 (Ar-C), 122.8 (Ar-C), 120.8 (Ar-C), 116.3 (CH), 115.1 (CH), 112.9 (Ar-C), 108.7 (Ar-C), 106.8 (Ar-C), 101.8 (CH₂), 56.0 (OCH₃), 40.3 (CH₂); HRMS (ESI-MS) *m/z*: [M + H]⁺ calcd for C₂₀H₁₈O₅⁺: 339.1229 found: 339.1224; IR (cm⁻¹): 2937 (OCH₃), 1704 (C=O), 1165 (Ar-C=C), 953, 946 (OCH₂).

3.2.2. Tyrosinase Inhibition and Kinetics Study

Compounds **c1**–**c29** were tested for their tyrosinase inhibitory activities according to previous reports [53,54]. Each compound was dissolved in DMSO and diluted to different concentrations. Tyrosinase and L-DOPA were dissolved in PBS solution (50 mM, pH 6.8). To 140 μL of tyrosinase (final concentration: 66.7 U/mL) solution, 10 μL of compound was added and incubated for 5 min at 25 °C, followed by the addition of 50 μL of L-DOPA (final concentration: 2 mM). Then, absorbance of the mixture was read at 475 nm. The inhibitory activity of each compound was calculated using DMSO as a blank control. Kojic acid was also used as the positive control.

The kinetics studies were carried out using the same experimental method as described above. For enzyme kinetics, the absorbance of the mixture containing different concentrations of tyrosinase (final concentration: 66.7 U/mL) and compound **c27** (0, 2, 3, and 4 μM) was recorded at 475 nm, respectively. For substrate kinetics, the absorbance of the mixture containing different concentrations of L-DOPA (final concentration: 2, 4, 6 and 8 mM) and compound **c27** (0, 2, 3 and 4 μM) was recorded at 475 nm, respectively.

3.2.3. Three-Dimensional Fluorescence Spectra Assay

The 3D fluorescence spectra of tyrosinase-compound **c27** mixture was measured according to previous reports [55]. To 3 mL of tyrosinase solution (final concentration: 168 μM) in PBS, 10 μL of compound **c27** (2 mM) was added and incubated for 5 min. Then, the 3D fluorescence spectra analyses were conducted in room temperature. The excitation and emission wavelengths were 200–600 nm and the slit width was 2.5 nm.

3.2.4. Circular Dichroism Spectroscopy Assay

The CD spectra of tyrosinase-compound **c27** mixture were measured according to previous reports [56]. To 190 μL of tyrosinase solution (final concentration: 64.65 μM) in PBS, 10 μL of compound **c27** (1.28, 2.56, and 3.84 mM) was added and incubated for 5 min. Then, the CD spectra were measured at 195–250 nm at room temperature.

3.2.5. Fluorescence Quenching Experiments

An amount of 1 μL of compound **c27** solution was titrated into 2 mL of tyrosinase and incubated for 5 min. Then, the fluorescence spectra were determined at excitation wavelength of 280 nm and temperatures of 303, 307, and 310 K, respectively. The quenching mechanism and parameters were investigated by the Stern–Volmer equation.

3.2.6. Molecular Docking

Molecular docking of tyrosinase–compound **c27** was conducted using SYBYL software according to previous reports [57–60]. Compound **c27** was treated with hydrogenation and energy minimization with the Gasteiger–Hückel program. The crystal structure of tyrosinase (PDBID: 2Y9X) was obtained from the RCSB Bank. Tyrosinase protein was analyzed with the internal program and we generated the active pocket using ligand mode. Then, the docking program was conducted in the default format to simulate the docking between tyrosinase and compound **c27**. In the docking process, 20 poses were generated for compound **c27**. We selected the pose with the highest score to further analyze the detailed interaction.

4. Conclusions

In this study, we synthesized cinnamic acid–eugenol esters **c1**–**c29** and assayed their tyrosinase inhibitory activities. The results showed that all cinnamic acid–eugenol esters **c1**–**c29** exhibited definite tyrosinase inhibitory activities. Compound **c27** was the strongest tyrosinase inhibitor ($IC_{50} = 3.07 \pm 0.26 \mu M$), and thus validated as a reversible mixed-type inhibitor against tyrosinase. Three-dimensional fluorescence and CD spectra results indicated that compound **c27** could change the conformation and secondary structure of tyrosinase. Fluorescence quenching results showed that compound **c27** quenched tyrosinase fluorescence in a static manner with one binding site. Molecular docking results also revealed the binding interactions between compound **c27** and tyrosinase. Therefore, cinnamic acid–eugenol esters, especially **c27**, could be used as lead compounds to find potential tyrosinase inhibitors.

Author Contributions: Conceptualization, X.X. and J.P.; investigation, J.L. and X.M.; writing and editing, X.X., X.Z., S.W. and J.L. All authors have read and agreed to the published version of the manuscript.

Funding: This research was supported by the Department of Education of Guangdong Province (Nos. 2021KCXTD044).

Institutional Review Board Statement: Not applicable.

Informed Consent Statement: Not applicable.

Data Availability Statement: Not applicable.

Conflicts of Interest: The authors declare no conflict of interest.

References

1. Li, J.; Feng, L.; Liu, L.; Wang, F.; Ouyang, L.; Zhang, L.; Hu, X.; Wang, G. Recent advances in the design and discovery of synthetic tyrosinase inhibitors. *Eur. J. Med. Chem.* **2021**, *224*, 113744. [[CrossRef](#)]
2. Hassan, M.; Shahzadi, S.; Kloczkowski, A. Tyrosinase inhibitors naturally present in plants and synthetic modifications of these natural products as anti-melanogenic agents: A review. *Molecules* **2023**, *28*, 378. [[CrossRef](#)] [[PubMed](#)]
3. He, M.; Fan, M.; Yang, W.; Peng, Z.; Wang, G. Novel kojic acid-1,2,4-triazine hybrids as anti-tyrosinase agents: Synthesis, biological evaluation, mode of action, and anti-browning studies. *Food Chem.* **2023**, *419*, 136047. [[CrossRef](#)] [[PubMed](#)]
4. Wang, G.; He, M.; Huang, Y.; Peng, Z. Synthesis and biological evaluation of new kojic acid-1,3,4-oxadiazole hybrids as tyrosinase inhibitors and their application in the anti-browning of fresh-cut mushrooms. *Food Chem.* **2023**, *409*, 135275. [[CrossRef](#)] [[PubMed](#)]
5. Lee, J.; Park, Y.J.; Jung, H.J.; Ullah, S.; Yoon, D.; Jeong, Y.; Kim, G.Y.; Kang, M.K.; Kang, D.; Park, Y.; et al. Design and synthesis of (Z)-2-(benzylamino)-5-benzylidenethiazol-4(5H)-one derivatives as tyrosinase inhibitors and their anti-melanogenic and antioxidant effects. *Molecules* **2023**, *28*, 848. [[CrossRef](#)]
6. Djafarou, S.; Mermer, A.; Barut, B.; Yilmaz, G.T.; Khodja, I.A.; Boulebd, H. Synthesis and evaluation of the antioxidant and anti-tyrosinase activities of thiazolyl hydrazone derivatives and their application in the anti-browning of fresh-cut potato. *Food Chem.* **2023**, *414*, 135745. [[CrossRef](#)]
7. Zargaham, M.K.; Ahmed, M.; Akhtar, N.; Ashraf, Z.; Abdel-Maksoud, M.A.; Aufy, M.; Nadeem, H. Synthesis, in silico studies, and antioxidant and tyrosinase inhibitory potential of 2-(substituted phenyl) thiazolidine-4-carboxamide derivatives. *Pharmaceuticals* **2023**, *16*, 835. [[CrossRef](#)]

8. Xue, S.; Li, Z.; Ze, X.; Wu, X.; He, C.; Shuai, W.; Marlow, M.; Chen, J.; Scurr, D.; Zhu, Z.; et al. Design, synthesis, and biological evaluation of novel hybrids containing dihydrochalcone as tyrosinase inhibitors to treat skin hyperpigmentation. *J. Med. Chem.* **2023**, *66*, 5099–5117. [[CrossRef](#)]
9. ZNajafi; Ebadi, A.; Chehardoli, G.; Ziaei, M.; Akbarzadeh, T.; Saeedi, M.; Gholamhoseini, P.; Mahdavi, M. Design, synthesis, in vitro, and in silico studies of novel benzylidene 6-methoxy-1-tetralone linked to benzyloxy and benzyl-1, 2, 3-triazole rings as potential tyrosinase inhibitors. *J. Mol. Struct.* **2023**, *1271*, 134018. [[CrossRef](#)]
10. BRoulier; Rush, I.; Lazinski, L.M.; Pérès, B.; Olleik, H.; Royal, G.; Fishman, A.; Maresca, M.; Haudecoeur, R. Resorcinol-based hemiindigoid derivatives as human tyrosinase inhibitors and melanogenesis suppressors in human melanoma cells. *Eur. J. Med. Chem.* **2023**, *246*, 114972. [[CrossRef](#)]
11. De Barros, M.R.; Menezes, T.M.; Garcia, Y.S.; Neves, J.L. Inhibitory effects of iron-based carbonaceous nanocomposites on mushroom tyrosinase activity: Molecular aspects and mechanistic insights. *New J. Chem.* **2023**, *47*, 9134–9142. [[CrossRef](#)]
12. Esma, A.T.K.; Abd, E.H.K.; Rabah, A.; Djamila, B.; Mohamed, S.B.; Chawki, B.; Ramazan, E. In vitro assessment of antioxidant, neuroprotective, anti-urease and anti-tyrosinase capacities of Tamarix africana leaves extracts. *J. Tradit. Chin. Med.* **2023**, *43*, 252–264. [[CrossRef](#)]
13. Romagnoli, R.; Oliva, P.; Prencipe, F.; Manfredini, S.; Germanò, M.P.; De Luca, L.; Ricci, F.; Corallo, D.; Aveic, S.; Mariotto, E.; et al. Cinnamic acid derivatives linked to arylpiperazines as novel potent inhibitors of tyrosinase activity and melanin synthesis. *Eur. J. Med. Chem.* **2022**, *231*, 114147. [[CrossRef](#)] [[PubMed](#)]
14. Su, J.; Li, D.; Hu, Y.; You, X.; Guo, X.; Li, X.; Chen, B. A novel C6-sulfonated celastrol analog as a tyrosinase and melanin inhibitor: Design, synthesis, biological evaluation and molecular simulation. *J. Mol. Struct.* **2023**, *1283*, 135–288. [[CrossRef](#)]
15. Nasab, N.H.; Raza, H.; Eom, Y.S.; Hassan, M.; Kloczkowski, A.; Kim, S.J. Synthesis and discovery of potential tyrosinase inhibitor of new coumarin-based thiophenyl-pyrazolylthiazole nuclei: In-vitro evaluation, cytotoxicity, kinetic and computational studies. *Chem. Biol. Drug. Des.* **2023**, *101*, 13–88.
16. Iraj, A.; Sheikhi, N.; Attaroshan, M.; Ardani, G.R.S.; Kabiri, M.; Bafghi, A.N.; Kobarfard, F.; Rezaei, Z.; Khoshneviszadeh, M.; Foroumadi, A.; et al. Design, synthesis, spectroscopic characterization, in vitro tyrosinase inhibition, antioxidant evaluation, in silico and kinetic studies of substituted indole-carbohydrazides. *Bioorganic Chem.* **2022**, *129*, 106–140. [[CrossRef](#)]
17. Ge, Z.; Liu, J.-C.; Sun, J.-A.; Mao, X.-Z. Tyrosinase Inhibitory Peptides from Enzyme Hydrolyzed Royal Jelly: Production, Separation, Identification and Docking Analysis. *Foods* **2023**, *12*, 2240. [[CrossRef](#)]
18. Güven, Z.B.; Saracoglu, I.; Nagatsu, A.; Yilmaz, M.A.; Basaran, A.A. Anti-tyrosinase and antimelanogenic effect of cinnamic acid derivatives from Prunus mahaleb L.: Phenolic composition, isolation, identification and inhibitory activity. *J. Ethnopharmacol.* **2023**, *310*, 116378. [[CrossRef](#)]
19. Ledwoń, P.; Goldeman, W.; Haldys, K.; Jewgiński, M.; Calamai, G.; Rossowska, J.; Papini, A.M.; Rovero, P.; Latajka, R. Tripeptides conjugated with thiosemicarbazones: New inhibitors of tyrosinase for cosmeceutical use. *J. Enzym. Inhib. Med. Chem.* **2023**, *38*, 2193676. [[CrossRef](#)]
20. Ielo, L.; Deri, B.; Germano, M.P.; Vittorio, S.; Mirabile, S.; Gitto, R.; Rapisarda, A.; Ronsisvalle, S.; Floris, S.; Pazy, Y. Exploiting the 1-(4-fluorobenzyl) piperazine fragment for the development of novel tyrosinase inhibitors as anti-melanogenic agents: Design, synthesis, structural insights and biological profile. *Eur. J. Med. Chem.* **2019**, *178*, 380–389.
21. Veljović, E.; Rimac, H.; Salihović, M.; Špirtović-Halilović, S.; Osmanović, A.; Kovač, N.; Kiršek, E.; Članjak-Kudra, E.; Špirtović, D.; Bojić, M. Synthesis of arylmethylene-bis (3-hydroxy-5, 5-dimethylcyclohex-2-en-1-one) derivatives and their effect on tyrosinase activity. *Croat. Chem. Acta.* **2021**, *94*, 1–9.
22. Chortani, S.; Hajlaoui, A.; Jilzi, S.; Harrath, A.H.; Jannet, H.B.; Romdhane, A. Access to new phosphonate-and imidazolidine-benzopyrimidinone derivatives as antityrosinase and anti-acetylcholinesterase agents: Design, synthesis and molecular docking. *J. Mol. Struct.* **2022**, *1268*, 133–693.
23. Mohammadsadeghi, N.; Mahdavi, A.; Saadati, F.; Mohammadi, F. In silico and in vitro studies of novel derivatives of tyrosol and raspberry ketone as the mushroom tyrosinase inhibitors. *Food Chem.* **2023**, *424*, 136413. [[CrossRef](#)]
24. Vittorio, S.; Dank, C.; Ielo, L. Heterocyclic Compounds as Synthetic Tyrosinase Inhibitors: Recent Advances. *Int. J. Mol. Sci.* **2023**, *24*, 9097. [[CrossRef](#)]
25. Zhu, Y.-Z.; Chen, K.; Chen, Y.-L.; Zhang, C.; Xie, Y.-Y.; Hider, R.C.; Zhou, T. Design and synthesis of novel stilbene-hydroxypyridinone hybrids as tyrosinase inhibitors and their application in the anti-browning of freshly-cut apples. *Food Chem.* **2022**, *385*, 132730. [[CrossRef](#)] [[PubMed](#)]
26. Yang, R.-L.; Chen, X.; Song, Y.-Y.; Zhu, Q.-L.; Bilal, M.; Wang, Y.; Tong, Z.; Wu, T.-T.; Wang, Z.-Y.; Luo, H.-Z.; et al. Whole cell-mediated biocatalytic synthesis of helioid cinnamylate and its biological evaluation as a novel tyrosinase inhibitor. *Biotechnol. Bioprocess Eng.* **2022**, *27*, 443–450. [[CrossRef](#)]
27. Nazir, Y.; Rafique, H.; Roshan, S.; Shamas, S.; Ashraf, Z.; Rafiq, M.; Tahir, T.; Qureshi, Z.-U.; Aslam, A.; Bin Asad, M.H.H. Molecular Docking, Synthesis, and Tyrosinase Inhibition activity of acetophenone amide: Potential inhibitor of melanogenesis. *BioMed. Res. Int.* **2022**, *2022*, 1040693. [[CrossRef](#)] [[PubMed](#)]
28. Cui, Y.; Hu, Y.-H.; Yu, F.; Zheng, J.; Chen, L.-S.; Chen, Q.-X.; Wang, Q. Inhibition kinetics and molecular simulation of p-substituted cinnamic acid derivatives on tyrosinase. *Int. J. Biol. Macromol.* **2017**, *95*, 1289–1297. [[CrossRef](#)]

29. Vale, J.A.D.; Rodrigues, M.P.; Lima, M.A.; Santiago, S.S.; Lima, G.D.d.A.; Almeida, A.A.; de Oliveira, L.L.; Bressan, G.C.; Teixeira, R.R.; Machado-Neves, M. Synthesis of cinnamic acid ester derivatives with antiproliferative and antimetastatic activities on murine melanoma cells. *Biomed. Pharmacother.* **2022**, *148*, 112–689. [[CrossRef](#)]
30. Neto, C.F.G.; Nascimento, P.D.; da Silveira, V.C.; de Mattos, A.B.N.; Bertol, C.D. Natural sources of melanogenic inhibitors: A systematic review. *Int. J. Cosmet. Sci.* **2022**, *44*, 143–153. [[CrossRef](#)]
31. Larik, F.A.; Saeed, A.; Channar, P.A.; Muqadar, U.; Abbas, Q.; Hassan, M.; Seo, S.-Y.; Bolte, M. Design, synthesis, kinetic mechanism and molecular docking studies of novel 1-pentanoyl-3-arylthioureas as inhibitors of mushroom tyrosinase and free radical scavengers. *Eur. J. Med. Chem.* **2017**, *141*, 273–281. [[CrossRef](#)]
32. Peng, Z.; Wang, G.; Zeng, Q.-H.; Li, Y.; Liu, H.; Wang, J.J.; Zhao, Y. A systematic review of synthetic tyrosinase inhibitors and their structure-activity relationship. *Crit. Rev. Food Sci.* **2021**, *62*, 4053–4094. [[CrossRef](#)]
33. Ashooriha, M.; Khoshneviszadeh, M.; Khoshneviszadeh, M.; Rafiei, A.; Kardan, M.; Yazdian-Robati, R.; Emami, S. Kojic acid–natural product conjugates as mushroom tyrosinase inhibitors. *Eur. J. Med. Chem.* **2020**, *201*, 112480. [[CrossRef](#)] [[PubMed](#)]
34. Cabezudo, I.; Ramallo, I.A.; Alonso, V.L.; Furlan, R.L. Effect directed synthesis of a new tyrosinase inhibitor with anti-browning activity. *Food Chem.* **2021**, *341*, 128232. [[CrossRef](#)] [[PubMed](#)]
35. Hariri, R.; Saeedi, M.; Akbarzadeh, T. Naturally occurring and synthetic peptides: Efficient tyrosinase inhibitors. *J. Pept. Sci.* **2021**, *27*, e3329. [[CrossRef](#)] [[PubMed](#)]
36. Obaid, R.J.; Mughal, E.U.; Naeem, N.; Sadiq, A.; Alsantali, R.I.; Jassas, R.S.; Moussa, Z.; Ahmed, S.A. Natural and synthetic flavonoid derivatives as new potential tyrosinase inhibitors: A systematic review. *RSC Adv.* **2021**, *11*, 22159–22198. [[CrossRef](#)]
37. Sheng, Z.; Ge, S.; Xu, X.; Zhang, Y.; Wu, P.; Zhang, K.; Xu, X.; Li, C.; Zhao, D.; Tang, X. Design, synthesis and evaluation of cinnamic acid ester derivatives as mushroom tyrosinase inhibitors. *MedChemComm* **2018**, *9*, 853–861. [[CrossRef](#)]
38. Citarella, A.; Moi, D.; Pedrini, M.; Pérez-Peña, H.; Pieraccini, S.; Dimasi, A.; Stagno, C.; Micale, N.; Schirmeister, T.; Sibille, G.; et al. Synthesis of SARS-CoV-2 Mpro inhibitors bearing a cinnamic ester warhead with in vitro activity against human coronaviruses. *Org. Biomol. Chem.* **2023**, *21*, 3811. [[CrossRef](#)]
39. Huang, S.; Liu, W.; Li, Y.; Zhang, K.; Zheng, X.; Wu, H.; Tang, G. Design, Synthesis, and Activity Study of Cinnamic Acid Derivatives as Potent Antineuroinflammatory Agents. *ACS Chem. Neurosci.* **2021**, *12*, 419–429. [[CrossRef](#)]
40. Jiang, Y.-Y.; Wu, S.; Wu, Y.-W.; Gao, Y.; Chong, D.; Sun, C.; Wei, M.-Y.; Gu, Y.-C.; Shao, C.-L.; Gu, Y. New brefeldin A-cinnamic acid ester derivatives as potential antitumor agents: Design, synthesis and biological evaluation. *Eur. J. Med. Chem.* **2022**, *240*, 114598. [[CrossRef](#)]
41. Wang, S.; Chen, J.; Shi, J.; Wang, Z.; Hu, D.; Song, B. Novel cinnamic acid derivatives containing the 1,3,4-oxadiazole moiety: Design, synthesis, antibacterial activities, and mechanisms. *J. Agric. Food Chem.* **2021**, *69*, 11804–11815. [[CrossRef](#)]
42. de Moraes, M.C.; Medeiros, G.A.; Almeida, F.S.; Rocha, J.d.C.; Perez-Castillo, Y.; Keesen, T.d.S.L.; de Sousa, D.P. Antileishmanial activity of cinnamic acid derivatives against *Leishmania infantum*. *Molecules* **2023**, *28*, 2844. [[CrossRef](#)] [[PubMed](#)]
43. Nazir, Y.; Saeed, A.; Rafiq, M.; Afzal, S.; Ali, A.; Latif, M.; Zuegg, J.; Hussein, W.M.; Fercher, C.; Barnard, R.T.; et al. Hydroxyl substituted benzoic acid/cinnamic acid derivatives: Tyrosinase inhibitory kinetics, anti-melanogenic activity and molecular docking studies. *Bioorg. Med. Chem. Lett.* **2020**, *30*, 126722. [[CrossRef](#)] [[PubMed](#)]
44. Tang, K.; Jiang, Y.; Zhang, H.; Huang, W.; Xie, Y.; Deng, C.; Xu, H.; Song, X.; Xu, H. Design, synthesis of cinnamyl-paeonol derivatives with 1, 3-dioxypropyl as link arm and screening of tyrosinase inhibition activity in vitro. *Bioorg. Chem.* **2021**, *106*, 104512. [[CrossRef](#)]
45. Lin, Z.; Xia, W.; Liu, R.; Jiang, S.; Ma, Z. Synthesis of cinnamic acid-coumarin ester analogs and inhibition of tyrosinase activity. *Chin. J. Org. Chem.* **2020**, *40*, 2980. [[CrossRef](#)]
46. He, M.; Fan, M.; Liu, W.; Li, Y.; Wang, G. Design, synthesis, molecular modeling, and biological evaluation of novel kojic acid derivatives containing bioactive heterocycle moiety as inhibitors of tyrosinase and antibrowning agents. *Food Chem.* **2021**, *362*, 130241. [[CrossRef](#)]
47. Ali, A.; Ashraf, Z.; Kumar, N.; Rafiq, M.; Jabeen, F.; Park, J.H.; Choi, K.H.; Lee, S.; Seo, S.-Y.; Choi, E.H.; et al. Influence of plasma-activated compounds on melanogenesis and tyrosinase activity. *Sci. Rep.* **2016**, *6*, 21779. [[CrossRef](#)]
48. Mermer, A.; Demirci, S. Recent advances in triazoles as tyrosinase inhibitors. *Eur. J. Med. Chem.* **2023**, *259*, 115655. [[CrossRef](#)]
49. Lin, J.; Xiao, D.; Lu, L.; Liang, B.; Xiong, Z.; Xu, X. New β -carboline derivatives as potential α -glucosidase inhibitor: Synthesis and biological activity evaluation. *J. Mol. Struct.* **2023**, *1283*, 135279. [[CrossRef](#)]
50. Zhang, X.; Zheng, Y.-Y.; Hu, C.-M.; Wu, X.-Z.; Lin, J.; Xiong, Z.; Zhang, K.; Xu, X.-T. Synthesis and biological evaluation of coumarin derivatives containing oxime ester as α -glucosidase inhibitors. *Arab. J. Chem.* **2022**, *15*, 104072. [[CrossRef](#)]
51. Li, M.; Li, L.; Lu, L.; Xu, X.; Hu, J.; Peng, J.-B. Anti- α -glucosidase, SAR analysis, and mechanism investigation of indolo [1,2-b]isoquinoline derivatives. *Molecules* **2023**, *28*, 5282. [[CrossRef](#)] [[PubMed](#)]
52. Wu, X.-Z.; Zhu, W.-J.; Lu, L.; Hu, C.-M.; Zheng, Y.-Y.; Zhang, X.; Lin, J.; Wu, J.-Y.; Xiong, Z.; Zhang, K.; et al. Synthesis and anti- α -glucosidase activity evaluation of betulonic acid derivatives. *Arab. J. Chem.* **2023**, *16*, 104659. [[CrossRef](#)]
53. YHu, G.; Gao, Z.P.; Zheng, Y.Y.; Lin, J.; Wu, X.Z.; Zhang, X.; Zhou, Y.S.; Xiong, Z.; Zhu, D.Y. Synthesis and biological activity evaluation of 2-cyanopyrrole derivatives as potential tyrosinase inhibitors. *Front. Chem.* **2022**, *10*, 540.
54. Alizadeh, N.; Sayahi, M.H.; Iraj, A.; Yazzaf, R.; Moazzam, A.; Mobaraki, K.; Adib, M.; Attarrosan, M.; Larijani, B.; Rastegar, H.; et al. Evaluating the effects of disubstituted 3-hydroxy-1H-pyrrol-2(5H)-one analog as novel tyrosinase inhibitors. *Bioorg. Chem.* **2022**, *126*, 105876. [[CrossRef](#)]

55. Lu, L.; Zhang, X.; Kang, Y.; Xiong, Z.; Zhang, K.; Xu, X.; Bai, L.; Li, H. Novel coumarin derivatives as potential tyrosinase inhibitors: Synthesis, binding analysis and biological evaluation. *Arab. J. Chem.* **2023**, *16*, 104724. [[CrossRef](#)]
56. Fan, M.; Yang, W.; Peng, Z.; He, Y.; Wang, G. Chromone-based benzohydrazide derivatives as potential α -glucosidase inhibitor: Synthesis, biological evaluation and molecular docking study. *Bioorg. Chem.* **2023**, *131*, 106–276. [[CrossRef](#)]
57. Nunes, J.A.; Araújo, R.S.A.D.; Silva, F.N.D.; Cytarska, J.; Łączkowski, K.Z.; Cardoso, S.H.; Mendonça-Júnior, F.J.B.; Silva-Júnior, E.F.D. Coumarin-based compounds as inhibitors of tyrosinase/tyrosine hydroxylase: Synthesis, kinetic studies, and in silico approaches. *Int. J. Mol. Sci.* **2023**, *24*, 5216. [[CrossRef](#)]
58. Cui, Y.; Chen, M.; Lin, G.; Duan, W.; Li, Q.; Zou, R.; Cen, B. Synthesis, antifungal activity and molecular docking study of 1,3,4-thiadiazole-urea compounds containing gem-dimethylcyclopropane ring structure. *Chin. J. Org. Chem.* **2022**, *42*, 3784–3797.
59. Sun, C.; Zhang, F.; Zhang, H.; Li, P.; Jiang, L. Design, synthesis, fungicidal activity and molecular docking study of novel 2-(1-methyl-1h-pyrazol-4-yl)pyrimidine-4-carboxamides. *Chin. J. Org. Chem.* **2023**, *43*, 229–235. [[CrossRef](#)]
60. Hemachandran, H.; Jain, F.; Mohan, S.; Kumar, T.D.; Doss, G.P.C.; Ramamoorthy, S. Glandular hair constituents of *Mallotus philippinensis* Muell. fruit act as tyrosinase inhibitors: Insights from enzyme kinetics and simulation study. *Int. J. Biol. Macromol.* **2018**, *107*, 1675–1682. [[CrossRef](#)]

Disclaimer/Publisher’s Note: The statements, opinions and data contained in all publications are solely those of the individual author(s) and contributor(s) and not of MDPI and/or the editor(s). MDPI and/or the editor(s) disclaim responsibility for any injury to people or property resulting from any ideas, methods, instructions or products referred to in the content.